The Influence of Infill Orientation and Surface Machining on the Fatigue Performance of Additively Manufactured Carbon Fibre Reinforced Polymer

Raffay Sultan

Degrees Thesis
Mechanical and Sustainable Engineering
2023

Degrees Thesis

Raffay Sultan

The influence of infill orientation and surface machining on the fatigue performance of additively manufactured Carbon Fibre Reinforced Polymer (CFRP).

Arcada University of Applied Sciences: Mechanical and Sustainable Engineering, 2023.

Identification number:

26079

Commissioned by:

Arcada University of Applied Sciences

Abstract:

This study aims to investigate the influence of infill orientation and surface machining on the fatigue performance of additively manufactured Carbon Fibre Reinforced Polymer (CFRP). SolidWorks software was used for designing the tensile test specimen according to the dimensions of standard ISO 527-2/1A. Then it was additively manufactured with various infill orientations (0^0,30^0,45^0,60^0,90^0) using FDM 3D printing. Two sets of specimens were produced. The fatigue life of the first set of specimens was studied to determine how the infill orientation influences the fatigue life of this material. The second set was processed using machining and sanding to alter its surface roughness. The surface roughness values of both sets were measured which showed that the surface roughness of specimens generally decreased after processing. Then fatigue life of the processed specimens was also studied. Finally, the fatigue performance results of original and processed specimens were compared to study how the fatigue performance of this material is influenced after processing. Specimens with 90-degrees infill orientation survived the highest number of fatigue cycles for both original and processed specimens.

Keywords:

Additively Manufactured, Carbon Fibre Reinforced Polymer, Surface Roughness, Surface Machining, 3D Printing, Infill Orientation, Fatigue Life

Contents

List of Symbols

A	Area (m^2)
E	Youngs's Modulus (Pa)
F	Force (N)
ΔL	Change in Length (mm)
L	Original Length (mm)
Nf	Fatigue life
σ	Stress (Pa)
ε	Strain
Pa	Pascal

Abbreviations

PLA	Polylactic Acid
FDM	Fused Deposition Modelling
AM	Additive Manufacturing
CFRP	Carbon Fibre Reinforced Polymer

1. INTRODUCTION

1.1 Background

Additive manufacturing is one of the most common techniques used for prototyping and producing objects designed in CAD software. It is widely used in industries such as automotive, composites, health care, electronics and aerospace. It is a very convenient method of producing high-quality complex geometries at an affordable cost. To make this process more efficient a lot of research is being done to find out various ways to improve this even further.

There are some theses and research done in a quite similar area such as (Rouf et al., 2022) concerning the details on effects of various 3D printing process parameters on the mechanical properties. (Rana, 2022) focusing on the influence of infill direction on the low cycle fatigue testing of 3D printed PLA polymer but it did not relate it to surface roughness. Another research article (Du et al., 2022) deals with the screening of surface roughness during additive manufacturing. Another relatable thesis topic was done at Arcada, on the impact of printing orientation on the tensile properties of the 3D printed parts using FDM (Tran, 2019). There is another research article on the development of surface roughness from additive manufacturing processing parameters and postprocessing surface modification techniques (Ralls et al., 2022). Research in a quite similar area was done on ultrasonic fatigue analysis of 3D-printed carbon fibre-reinforced plastic (Jung et al., 2022). (Parandoush & Lin, 2017) is also another detailed review on the additive manufacturing of polymer-fibre composites and how to improve it further. In general, there is enough research done in the area of additive manufacturing, tensile properties of the polymer, fatigue life and surface roughness but this is a quiet new research made in this area. This thesis topic is quite distinct from the theses previously done, as it is quite specifically comparing the effect of surface machining on the fatigue life of additively manufactured carbon fibre reinforced polymer.

1.2 Objective

The objective of this thesis is to study the fatigue life of this material by varying the various conditions such as infill orientation. ColorFabb XT-CF20 a high-quality Eastman Amphora AM 1800 copolyester-based 3D printing filament, infused with 20% carbon fibres is used as a printing material. This thesis aims to study the fatigue life of this material based on surface roughness altered using surface machining and sanding.

- 3D printing of the specimens will be done using FDM printing technology with varying infill orientations (0^0,30^0,45^0,60^0,90^0).
- The high-cycle fatigue testing with low-stress amplitude loading will be done on both original and processed samples to investigate how these samples behave on fatigue life testing.
- It will be studied how many fatigue life cycles each sample can bear to draw out a conclusion on how the machining and sanding influences the fatigue life of additively manufactured copolyester-based 3D printing filament.

After obtaining all the data, the following will be explained in the discussion part:

- Influence of infill orientations on the fatigue life of the carbon fibre reinforced polymer.
- Influence of surface machining and change in surface roughness due to sanding on the fatigue life of the carbon fibre reinforced polymer.

Then in the conclusion part, it will be concluded how the machining and sanding influences the fatigue life of this material.

1.3 Relevance to the Degrees Programme

The Mechanical and Sustainable Engineering degrees programme has relevance to this thesis to a very high extent as it involves polymer processing, designing, 3D printing, mechanical testing and data analysis. These are among the main core study components of this study programme. From the perspective of Mechanical Engineering, it involves the testing of various mechanical properties of a composite material. Material is getting tested with various infill variations to determine the best possible optimization for additive manufacturing purposes.

2. LITERATURE REVIEW

2.1 Additive Manufacturing

Additive Manufacturing (also known as 3D printing) is one of the most common methods to produce solid objects from designs created in CAD software. AM summarizes all the technologies that produce objects layer by layer by using materials such as plastic or metal (*Am basics* 2022). Many individuals, even professionals in Additive Manufacturing (AM), use the phrases 3D printing and AM interchangeably when speaking generally. The word AM is frequently preferred for more in-depth or technical conversations, and it can be used to describe both the printing process and factors to be taken into account while finishing printed items.

Since the middle of the 1980s, 3D printing has made it possible for anyone to produce parts straight from digital design files. New three-dimensional 3D parts can now be produced in low to medium volumes easily than ever before due to the advancement in technology. By the 2000s, additive manufacturing (AM) technologies had advanced and were mostly used for commercial prototypes. Three brand-new, distinct additive manufacturing technologies achieved commercialization in 1991. Among those three, Fused Deposition Modelling(FDM) is a technology that was created by Scott Crump, who also established Stratasys. Solid ground curing is a technology that was unveiled by a firm called Cubital (SGC). Laminated Object Manufacturing (LOM) is an additive manufacturing technique that was developed by the company Helisys (*Additive manufacturing history: From the 1980's to now*). Making anything for the first time is one of the most challenging tasks. Making new things is where 3D printers shine. In fact, "rapid prototyping" by which the business was known for a few decades was an early popular usage for 3D printers.

Nowadays, AM is becoming faster and more dependable as well as a standard manufacturing technology for producing sophisticated parts in addition to prototypes. Freeform, attractive, and even complex designs that are impractical to be produced using moulds or castings yet can now be produced using AM. A significant growth engine in some of the biggest global sectors today is additive manufacturing. From the source

(*Additive manufacturing history: From the 1980's to now*), it is found that 47% of manufacturers employ additive manufacturing technology, including 22.1% of automotive manufacturers, 12.5% of product development firms, and 4.8% of medical manufacturers, according to the latest data on industry usage of 3D printing. Additive manufacturing is also being adopted at an ever-increasing rate in the aerospace, educational, and defence sectors.

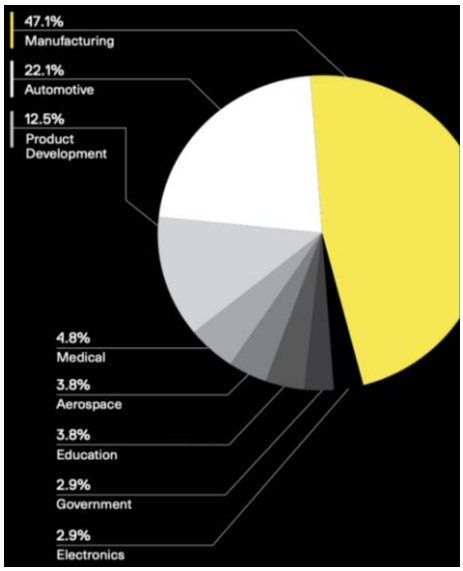

Figure 1: Adoption percentages of AM across various industries (Additive manufacturing history: From the 1980's to now)

2.1.1 Fused Deposition Modelling(FDM)

There are many types of AM technology but for this thesis work mainly Fused Deposition Modelling (FDM) is concerned. Fused deposition modelling(FDM) 3D printing, also known as fused filament fabrication (FFF), is a material extrusion additive manufacturing (AM) process. FDM constructs parts layer by layer by depositing melted material in a predetermined path (*What is FDM (fused deposition modeling) 3D printing?*). The final physical objects are formed using thermoplastic polymers in the form of filaments. FDM has the largest installed base of 3D printers worldwide. It is the most widely used technology across many industries around the globe (*What is FDM (fused deposition modeling) 3D printing?*).

An FDM 3D printer works by depositing melted filament material layer by layer over a build platform until you have a finished part. FDM works with digital design files that are uploaded to the machine and converted into physical dimensions. Polymers such as ABS, PLA, PETG, and PEI are used in FDM, and the machine feeds them as threads through a heated nozzle (*What is FDM (fused deposition modeling) 3D printing?*) .To use an FDM machine, first, insert a spool of thermoplastic filament into the printer. The printer feeds the filament through an extrusion head and nozzle once the nozzle reaches the desired temperature.

This extrusion head is connected to a three-axis system, allowing it to move along the X, Y, and Z axes. The printer extrudes melted material in thin strands and deposits it layer by layer along a design path. The material cools and solidifies after it is deposited. Multiple passes are required to fill an area, similar to colouring in a shape with a marker (*What is FDM (fused deposition modeling) 3D printing?*). When a layer is completed, the build platform descends and the machine moves on to the next layer. In some machine configurations, the extrusion head moves upward. This process is repeated until the part is completed.

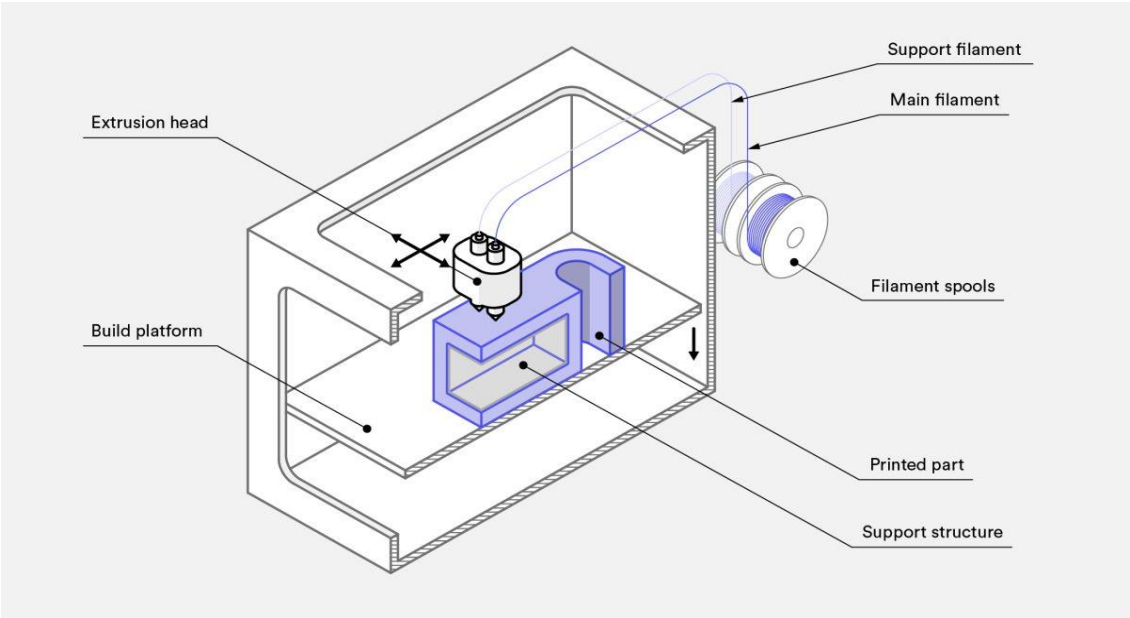

Figure 2: A typical FDM printer's schematic (What is FDM (fused deposition modeling) 3D printing?)

2.1.2 Printing Parameters

In FDM 3D Printing there is a lot of freedom to adjust printing parameters to get a desired geometry of the object. Most FDM systems allow you to change several process parameters. These include the temperatures of the nozzle and build platform, as well as the build speed, layer height, infill orientation, and cooling fan speed.

A typical desktop 3D printer build size is 200 x 200 x 200 mm, while industrial machines can reach 1000 x 1000 x 1000 mm. The typical layer height of the part getting printed using FDM is between 50 and 400 microns (*What is FDM (fused deposition modeling) 3D printing?*). Printing shorter layers produces smoother parts and captures curved geometries more accurately, whereas printing with high layer thickness allows you to create parts faster and at a lower cost.

2.1.3 Printing Materials

One of the primary benefits of using FDM is that a wide range of materials can be used as printing materials. For example, commodity thermoplastics like PLA and ABS are included. As well as engineering materials like PA, TPU, and PETG. High-performance thermoplastics like PEEK and PEI can also be printed. PLA filament is the most widely used material in desktop FDM printers. PLA printing is simple and can produce parts with finer details. Various materials are being used in the industry for 3D printing purposes according to the nature of the part application. Nowadays, various composite materials are also being used for 3D printing. Printing with different materials will affect the mechanical properties and accuracy of your part, as well as its cost. The figure 3 below is obtained from (*What is FDM (fused deposition modeling) 3D printing?*) compares the most common FDM materials:

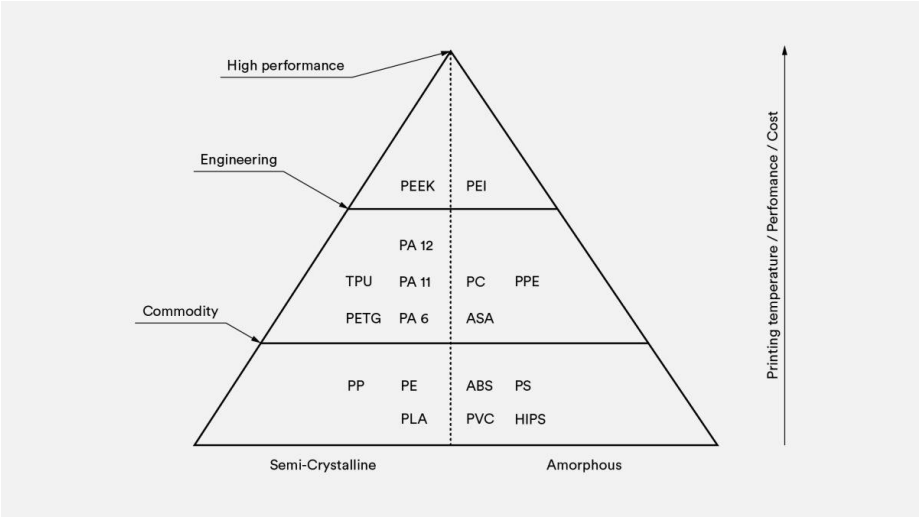

Figure 3 Commonly used FDM 3D printing materials (What is FDM (fused deposition modeling) 3D printing?)

2.1.4 Carbon Fibre Reinforced Polyester as a 3D printing material

Carbon fibre-reinforced composite materials are also being used in AM nowadays. One of the most common examples is XT-CF 20 a carbon fibre composite material loaded with 20% milled carbon fibres (*XT-CF20*) which is being used in this thesis work. It is a high-quality Eastman Amphora AM 1800 copolyester-based 3D printing filament, infused with 20% carbon fibres. This composite material is an excellent filament for parts which require high stiffness. Parts 3D printed using this material have a fine matt black finish when printed. It is a strong material with good properties capable of producing high-quality stiff parts. The typical properties of this material, when 3D printed, can be found in the table below obtained from the source (*XT-CF20*):

Table 1 Properties of XT-CF 20

Properties	**Value**	**Method**
Tensile Modulus	5143 MPa	ISO 527
Tensile Strength	55.78 MPa	ISO 527
Tensile Strain at tensile strength	2.04 %	ISO 527
Tensile Stress at break	55.78 MPa	ISO 527
Tensile Strain at break	2.04 %	ISO 527
Diameter	1.75 mm	
Filament weight	750 g	

Figure 4: ColorFabb XT-CF 20 Spool (XT-CF20)

2.2 Tensile Properties

The tensile property can be defined as the reaction of the material to resist, when tension forces are applied to it (*Tensile property* 2019). Determination of the tensile properties of the material plays a great role in Mechanical Engineering and Material Processing. It is important to determine the tensile properties since doing so can give information regarding the elastic limit, elongation, proportional limit, reduction in area, tensile strength, yield point, yield strength, and other tensile properties. When the tensile properties are known, it becomes easier to decide where the material can be applied. Tensile testing yields a load versus elongation curve, which is then transformed into a stress vs strain curve to determine the tensile properties, which vary from material to material. Generally, tensile testing is used to determine tensile properties.

2.2.1 Tensile Stress

When a force is applied to a specific cross-sectional area of an object, the loading is expressed in terms of stress (*Stress and strain*). It can be summarized as the force acting per unit area. Stress is the force exerted or a combination of forces that tends to deform a body from the perspective of loading. Depending on the type of loading, the applied stress may or may not be uniform. For instance, a bar loaded fully in tension will effectively have a uniform distribution of tensile stress. A bar loaded for bending, however, will show a stress distribution that varies with the distance perpendicular to the normal axis. There are usually three components to the internal force acting on a certain area of a plane. One normal to the plane and two parallel to the plane. The normal stress is

calculated by dividing the normal force component by the area, and the shear stress is calculated by dividing the parallel force components by the area. Stress has a unit of Pascal (Pa).

$$\sigma = \frac{Force}{Cross-Sectional\ Area} = \frac{F}{A} \quad \ldots\ldots\ldots\ldots\ldots\ldots\ldots\ldots \quad (1)$$

2.2.2 Tensile Strain

When a material is subjected to force, it creates stress, which causes deformation. This deformation which causes a change in length is called strain (*Stress and strain*). Engineering strain is determined by dividing the amount of deformation in the direction of the applied force by the material's original length. Strain as a quantity has no unit. For instance, the strain in a bar stretched under tension is equivalent to the amount of extension or change in length divided by the bar's initial length. Similar to stress, a complex structural element's strain distribution may or may not be uniform depending on the type of loading.

$$\varepsilon = \frac{Change\ in\ Length}{Original\ Length} = \frac{\Delta L}{L_0} \ldots\ldots\ldots\ldots\ldots\ldots\ldots\ldots\ldots\ldots\ldots\ldots\ldots\ldots (2)$$

2.2.3 Young's Modulus

Young's modulus, a numerical constant named after the 18th-century English physician and physicist Thomas Young, it describes the elastic properties of a solid undergoing tension or compression in only one direction (*Young's Modulus* 2023). As in the case of a metal rod that, after being stretched or compressed lengthwise, returns to its original length. In simple words, it can be defined as a ratio of stress and strain. Young's modulus is a measurement of a material's capability to endure deformations when placed under tension or compression along its length. Young's modulus is also referred to as the modulus of elasticity. It is determined by dividing the longitudinal stress by the strain. It has a unit of (N/m^2) or Pascals (Pa). Young's modulus is only significant in the region where the stress is proportional to the strain and the material recovers to its initial form

upon removal of the external force. As the tensions rise, the material may either flow, permanently change its shape or finally break.

$$E=\frac{Stress}{Strain}=\frac{\sigma}{\varepsilon} \quad \text{.....(3)}$$

$$\sigma = Stress\ (Pa)$$

$$\varepsilon = Strain$$

E is the Young's Modulus (Pa) in the equation above.

2.3 Surface Roughness

The term surface roughness, indicates the tiny, closely spaced deviations from the nominal surface resulting from the characteristics of the material and process of manufacturing (*surface roughness in manufacturing - LEADRP* 2022). The surface is considered rough if these variations are large and smooth if they are moderate. Roughness is generally perceived in surface metrology as the high-frequency, short-wavelength component of a measured surface. The relative roughness of a surface profile is usually calculated using the numerical parameter Ra to obtain surface roughness. Ra is the arithmetic mean of surface height deviations determined over a surface. Surface profile measuring equipment such as a profilometer can determine surface roughness. It is the deviation of a mean line from the average height of part roughness irregularities. In many engineering applications, it may have a major impact on the durability and performance of parts.

In comparison to smooth surfaces, rough surfaces have higher coefficients of friction and wear faster. Since flaws serve as the nucleation sites for breakage or cracks, surface roughness is a reliable indicator of mechanical part performance. While manufacturing a product usually, Engineers and producers determine the required level of surface roughness according to the application of the material. It assists in the development of reliable products and consistent processes. Surface Roughness, also known as surface texture or surface topography, is a phrase that refers to the general quality and smoothness of a surface. It takes into account a surface's minute, local deviations from the ideal flatness (a proper plane). Lay, waviness, flaws, and roughness are the four characteristics

that make up a surface texture. The most commonly utilized description of a surface finish's characteristic is roughness.

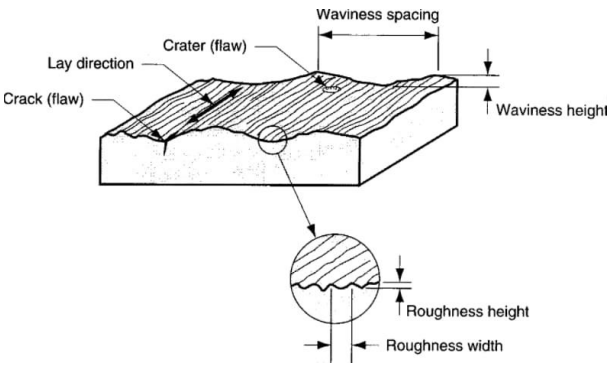

Figure 5 Relationship between lay, waviness, defects and roughness (surface roughness in manufacturing - LEADRP 2022)

2.4 Fatigue Life

A specimen's fatigue life is the number of loading (stress or strain) cycles it can tolerate before failing in a certain way (*What is fatigue life?*). Fatigue is the progressive localized permanent structural change that takes place in a material when it is exposed to conditions that cause fluctuating loads and strains at some region or areas and that, after a sufficient number of fluctuations, may lead to cracks or full fracture. In fatigue testing, it is the requirement for fluctuating (repeated or cyclic) loads to act under either constant amplitude or variable amplitude. As the material is repeatedly loaded and unloaded, fatigue develops. Microscopic cracks will start to appear around the areas that have stress concentration, such as the surface. After several fatigue cycles when load exceeds a particular threshold, cracks start to appear. This is the Ni phase of crack initiation. A crack will eventually grow to a critical size, suddenly spread, and fracture the structure. This is Np, the phase of fracture propagation. The two stages are added together to create the total fatigue life (Nf).

$$N_f = N_i + N_p \quad \text{.....(4)}$$

Where N_f = Total Fatigue Life

N_i = Crack Initiation Phase

N_p = Crack Propagation Phase

It is crucial to understand the differences between stress range, stress amplitude, and maximum stress in fatigue life analysis. Instead of the maximum stress, what causes fatigue damage is the stress range (i.e., the variability of the stresses) (*What is fatigue life?*). Stress amplitude and mean stress are crucial factors in fatigue life analysis.

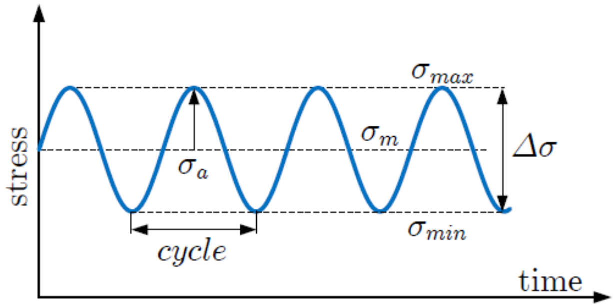

Figure 6 Stress range, max and min stress (What is fatigue life?)

$$\Delta\sigma = \sigma max - \sigma min \quad \ldots\ldots(5)$$

Where $\Delta\sigma$= Stress Range

σmax= Maximum Stress

σmin= Minimum Stress

The effective mean stress is the ratio of the stresses:

$$R=\frac{\sigma max}{\sigma min} \quad \ldots\ldots(6)$$

There are two types of stress loadings Constant Amplitude loading and Variable Amplitude loading as seen in the figure below:

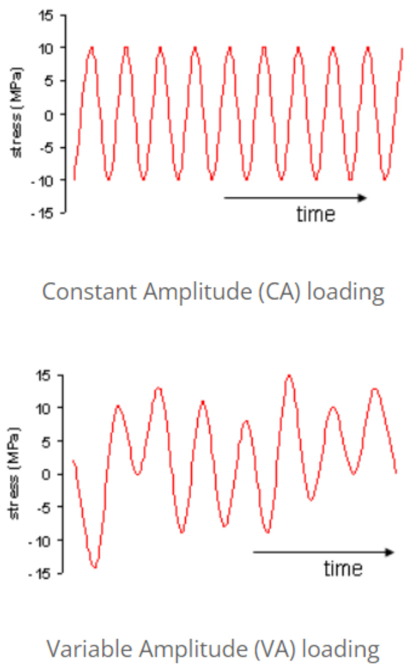

Figure 7 Constant and Variable Amplitude Loading (What is fatigue life?)

There are two main types of fluctuating stresses:

1. Completely Reversed Stress:

In this type of stress, the half cycle is on tensile stress and the remaining half consists of compressive stress, therefore the mean stress is zero (*Special cases of fluctuating stresses*).

$$\sigma min = -\sigma max \quad \text{.....(7)}$$

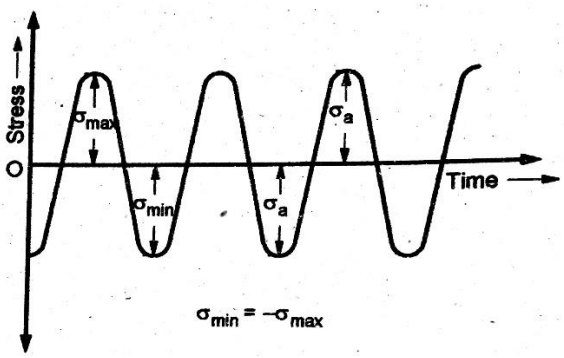

*Figure 8 Reversed Stress (*Special cases of fluctuating stresses*).*

2. Repeated Stress:

Stresses that vary from zero to a certain maximum value are called repeated stresses. The minimum stress is zero in this specific case so mean stress and amplitude stress have equal values (*Special cases of fluctuating stresses*).

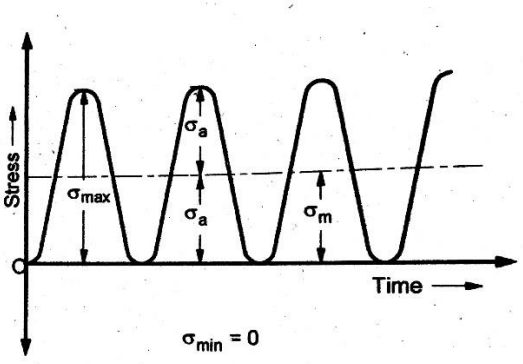

Figure 9 Repeated Stress (Special cases of fluctuating stresses).

3. METHOD

3.1 Specimen Design

SolidWorks is one of the most commonly used CAD designing software. It is an efficient tool for designing objects, visual creativity, modelling, project management and carrying out various types of simulations. The tensile test specimen used in this thesis work is designed in SolidWorks according to the dimensions given in standard ISO 527-2/1A. The design dimensions of the specimen are shown in figure 10 and table 2 below:

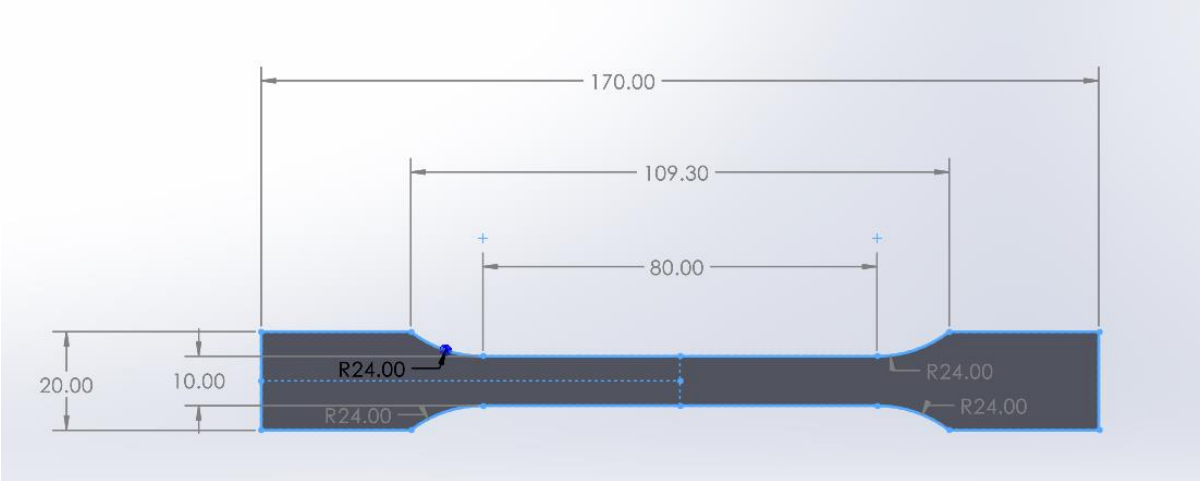

Figure 10 Specimen Dimensions

Table 2 Dimensions of the Specimen

Dimensions	**Values (mm)**
l_3	170
l_2	109.30
l_1	80
b_1	10
b_2	20
r	24
h (thickness)	4

The specimen was designed carefully and then extruded out 4 mm. The final image of the completed specimen can be seen in figure 11:

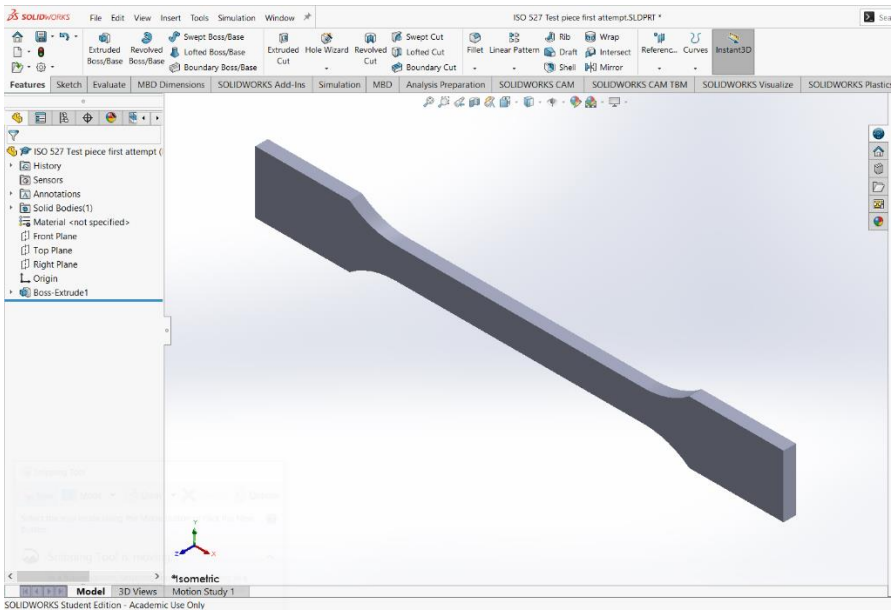

Figure 11 Designed Specimen in SolidWorks

3.2 Specimen Print Settings

Print settings play a great role in AM as they determine the print quality of the object. They need to be adjusted as every 3D printer, every material and object is different from others, so they need custom print settings to produce a quality print (*The best 3D printer settings for perfect prints* 2022). Carbon fibre reinforced polyester was stiffer than most of the 3D printing materials so needed custom print settings to produce good quality prints, which were figured out by making various trial and error attempts. Print speed was kept low so that material can flow slowly out of the nozzle to improve the bed adhesion. Print and bed temperatures were also kept high to ensure proper adhesion of the material to the bed. Samples were printed with various infill directions (0^0,30^0,45^0,60^0,90^0). The samples were printed at standard quality according to Cura software settings. The total thickness of each specimen was 4 mm. The top and bottom both were 0.4 mm each containing two layers of 0.2 mm. Which in total becomes 0.8 mm including top and bottom, in between 3.2 mm was infill with varying orientations. The skirt was used as an adhesion assistant to ensure the material is flowing smoothly through the nozzle before printing the first critical layer of the sample. The print settings used are mentioned in the table 3 :

Table 3 Print Settings

Print Setting	Value
Layer Height	0.2 mm
Top bottom thickness	0.4 mm
Top Thickness	0.4 mm
Top Layers	2
Bottom Thickness	0.4 mm
Bottom Layers	2
Infill Density	100 %
Infill Pattern	Lines
Infill Line Directions	0^0,30^0,45^0,60^0,90^0
Printing Temperature	270^0C
Build Plate Temperature	75^0C
Print Speed	40 mm/s

3.3 Slicing Software (Cura)

After the part has been successfully designed in CAD software, it can be converted into a real object using additive manufacturing in this process intermediate software is required which was in this case, Ultimaker Cura. CAD file was saved in STL format to be processed by Cura. STL file was then opened in Cura, where the object is sliced to form a G-code to be understood by the 3D printer. Finally, the G-code file was sent to the 3D printer and it started to print the part layer by layer according to the G-code instructions.

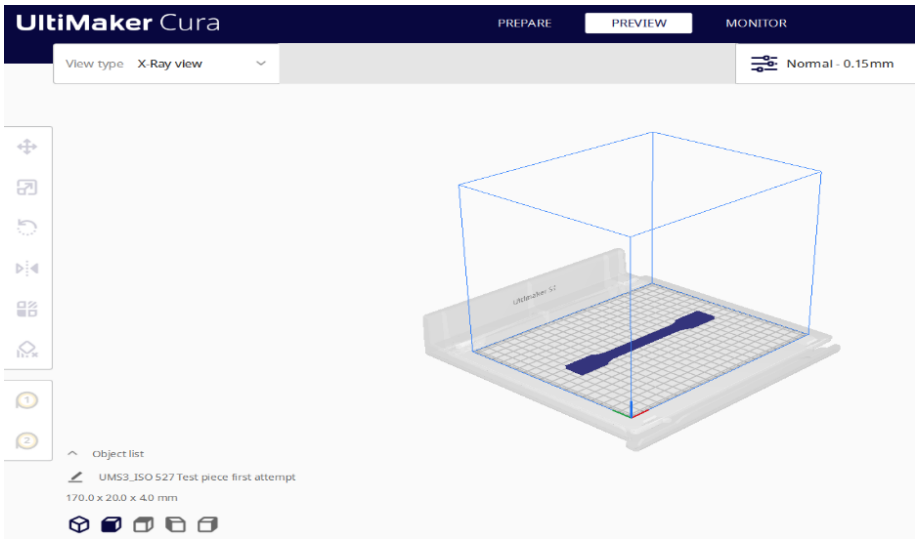

Figure 12 Sliced Specimen in Ultimaker Cura Software

3.4 3D Printer used in Printing Process:

The 3D printer used for the additive manufacturing of these specimens is Creality Ender-3 S1 Pro. It uses FDM (Fused Deposition Modelling) technology for printing which is one of the most commonly used 3D printing technology for conventional 3D printing. It is user-friendly and easy to use. It is well known for its high-temperature printing possibilities of up to 300^0C using its brass nozzle. It has many advanced features such as auto-bed leveling, touch screen interface along with smooth feeding using a sprite full metal dual gear direct extruder having an extrusion force of 80 N to ensure smooth feeding (*Ender-3 S1 Pro 3D Printer*). It is compatible with multiple filaments such as PLA, ABS, PVA, PETG, PA and many other composite materials which provide more possibilities to print various types of objects. It has a 4.3-inch touchscreen for controls such as adjusting printing parameters. It has a 32-bit fast-processing motherboard with low-level noise exposure. It is equipped with CR Touch, the 16-point levelling which ensures proper leveling of the bed to provide high-quality prints. The printing parameters were adjusted several times until the samples printed with high quality started to appear. The image of the printer while printing can be seen below in figure 13 along with the printer properties in table 4:

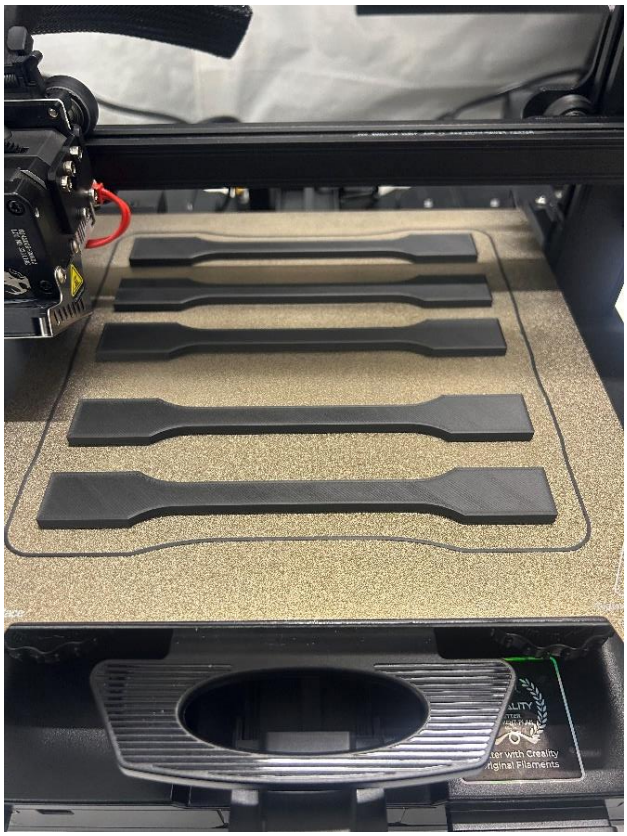

Figure 13 Creality Ender-3 S1 Pro 3D Printer

Table 4 Printer properties

Properties	Values
Model	Ender-3 S1 Pro
CAD Software	SolidWorks
Printing Technology	FDM
Machine Build Volume	220x220x270 mm
Assembled Dimensions	490x455x625 mm
Net Weight	8.7 kg
Compatible Diameter	1.75 mm
Nozzle Temperature	Upto 300^0C
Bed Temperature	Upto 110^0C

3.5 Infill Orientation

The specimens were 3D printed with varying infill orientations (0^0,30^0,45^0,60^0,90^0). The reason for this is to have a better understanding of how the infill orientation of a

specific specimen affects its fatigue life. Two sets of tensile test pieces were prepared. The fatigue life of the first set of specimens having various infill orientations was studied. Whereas the other one was processed using machining and sanding. Later the fatigue life of processed samples was studied. Then later comparison was done to investigate how the machining and sanding has affected the fatigue life of the samples, printed with varying infill orientations.

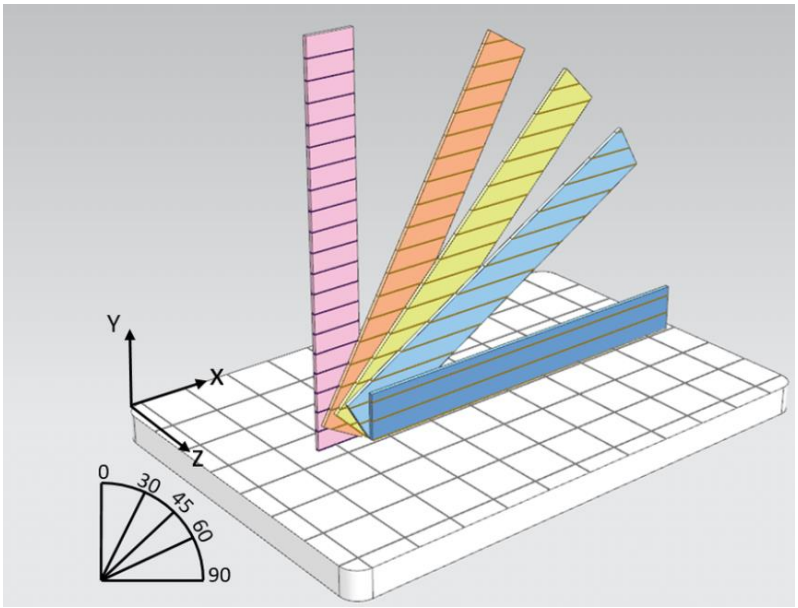

Figure 14 Infill orientations (Samples with printing orientations 0 • , 30 • , 45 • , 60 • and 90)

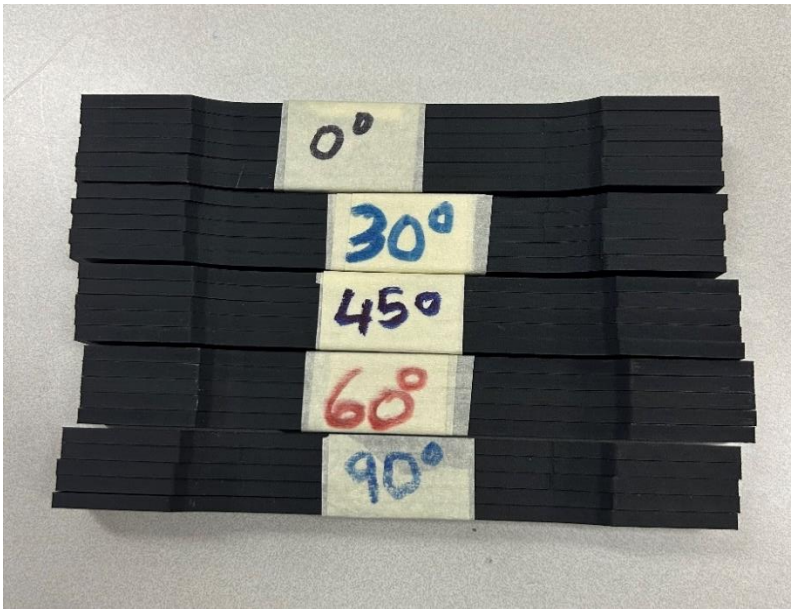

Figure 15 Printing of the Specimens with varying orientations

3.6 Machining and Sanding of the Specimens

After the printing of the specimens was completed in all the printing orientations, some of the samples were separated to be used in their original form and others were separated so that their roughness profile can be altered by processing. The outer appearance of the printed samples was a little bit different on the top and bottom due to the high temperature of the bed at the bottom. The appearance of the original specimen can be seen in figures 16 and 17 below:

Figure 16 Top of the Original Specimen

Figure 17 Bottom of the Original Specimen

Then the roughness profile of the specimens was altered using the processes of Machining and Sanding. The processes used for altering the roughness profile of the specimens are mentioned below:

- Firstly, machining was done using the 16 mm end mill using the HAAS CNC milling machine at the middle-reduced section of the specimen from both the top and bottom sides for about 0.25 mm each.
- After that sanding was done 25 times on each surface using sand paper under constant conditions.

This way the roughness profile of the original samples was altered, and later surface roughness testing was done using surface roughness testing machine. This is how the specimens were processed using machining and sanding to alter their roughness profile.

Surface roughness testing was done to get the surface roughness values of both processed and unprocessed samples to later study how samples with various surface roughness values are performing at fatigue life testing. The appearance of the processed sample was different from the original sample as it can be seen in the figures 18 and 19 below:

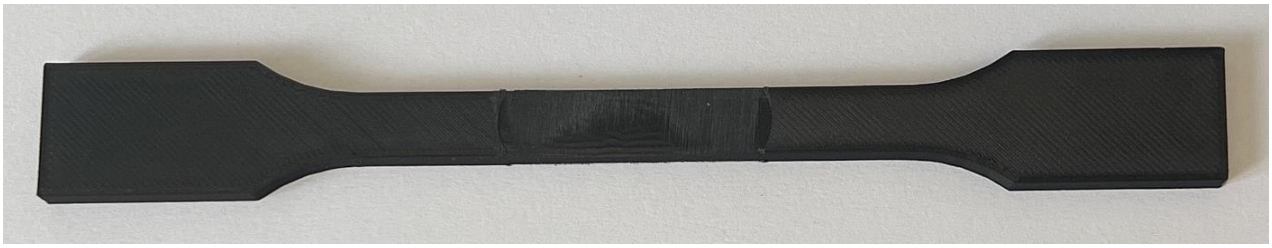

Figure 18 Top of the Processed Specimen

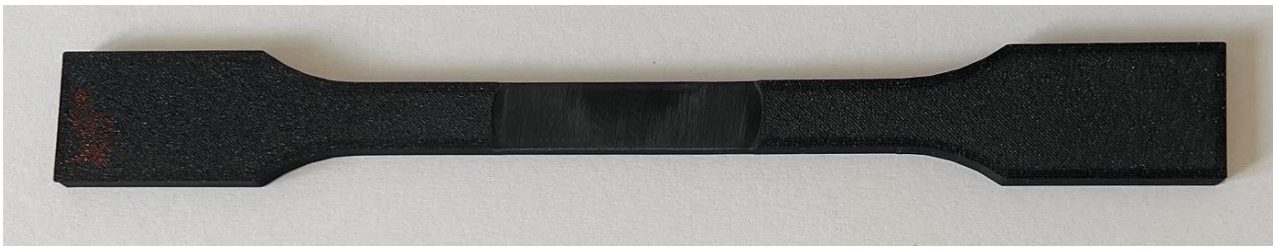

Figure 19 Bottom of the Processed Specimen

3.7 Fatigue Life Testing

The machine used for fatigue life testing of these specimens is Testometric X350-20, it is a fully digital testing system with high precision, control and accuracy (*X350 – in quality*). The same testing was repeated for all specimens of (0^0,30^0,45^0,60^0,90^0) degrees. Testing parameters remained the same for all the tests. It supports various types of tensile testing and provides precise results with very high accuracy. It can be seen in the figure 20 shown below:

Figure 20 Testometric X350-20 Tensile Testing Machine (X350 – in quality)

4. RESULTS

4.1 Surface Roughness Testing

Surface roughness testing of the specimens was done using Mitutoyo SURFTEST SJ-410, surface roughness testing machine (*SURFTEST SJ-410 series* 2022). It is an excellent equipment which provides very accurate values for the roughness of different surfaces. Surface roughness testing was done for all the samples to obtain Ra, Rq and Rz values.

Figure 21 Mitutoyo SJ-410 (SURFTEST SJ-410 series 2022)

4.1.1 Surface Roughness Testing of Original Specimens

For the surface roughness measurement of the specimens, it was noticed that the top and bottom of the specimens have different values of roughness as the high temperature of the bed changes the texture of the bottom to some extent. So, it was concluded that the surface roughness of both the top and bottom should be measured to have an average value of surface roughness. To make the testing results even more accurate, two samples of each angle variation were tested. The average values of tops and bottoms were considered for the calculation of the final average surface roughness value of that specimen. After getting the top and bottom roughness values of each specimen, their average was taken to get the overall roughness value of that specimen. The roughness profile data was little bit different for both the top and bottom. To illustrate how the graphs appeared , the graphs for 0^0 are shown below in figure 22 and 23:

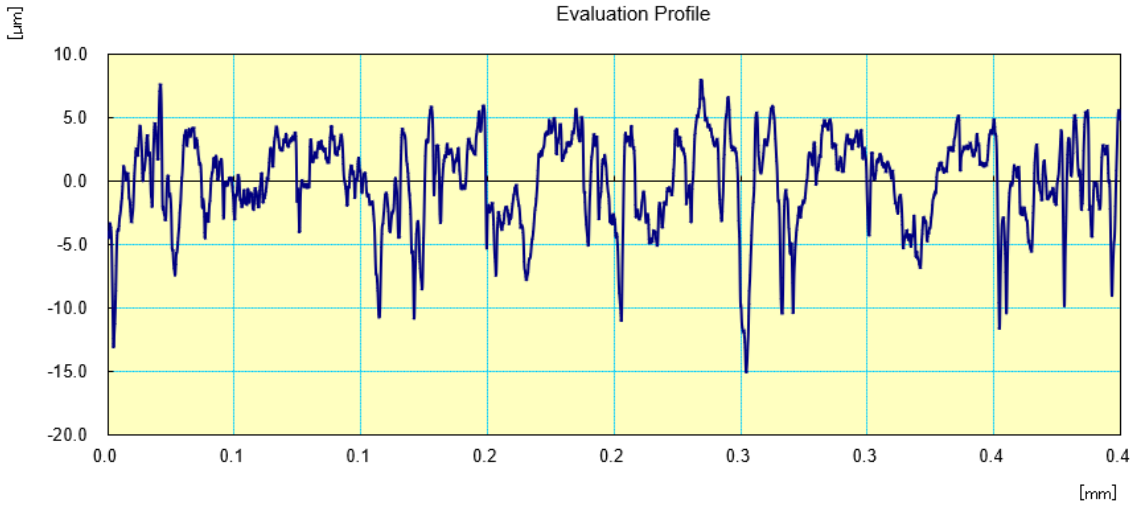

Figure 22 Surface Roughness Profile graph for 0-degrees specimen Top

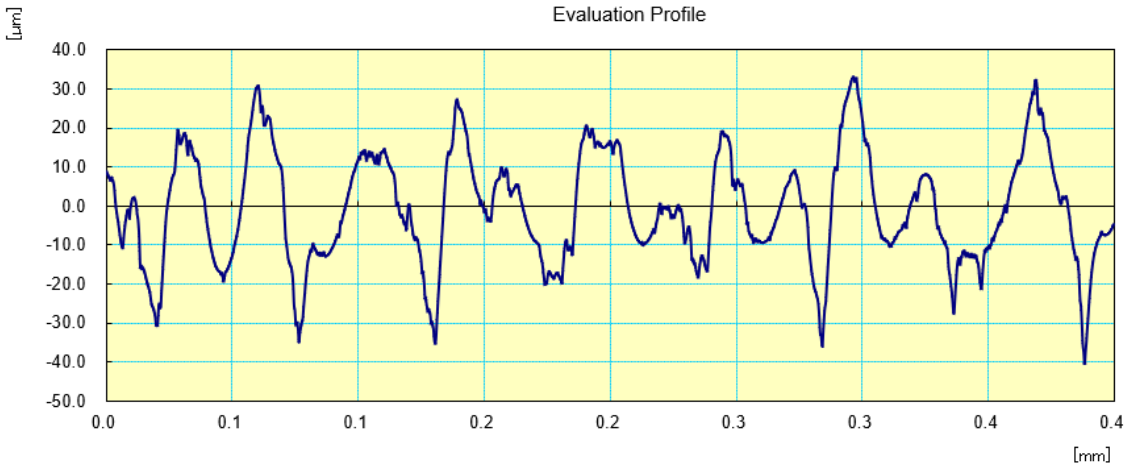

Figure 23 Surface Roughness Profile graph for 0-degrees specimen Bottom

As seen in the surface roughness profile figures 22 and 23 above, it can be seen that there is a slight variation in the roughness profiles of the top and bottom. That is why the roughness of both were measured and their average value was considered as the surface roughness of the sample. All the measurements were done from the middle-reduced section of the specimen mostly around the centre same place as where the roughness profile was altered on the processed specimens to have a fair comparison.

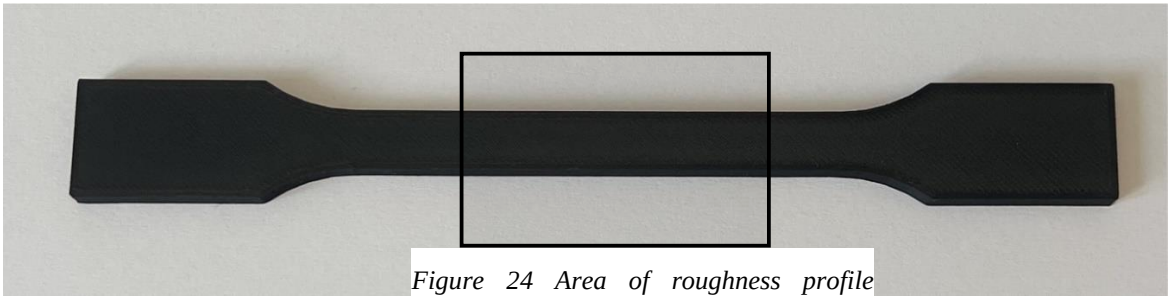

Figure 24 Area of roughness profile alteration

Figure 25 Specimen with area of testing and roughness profile alteration outlined

In figure 25 above, the marked area can be seen where the roughness profile was altered through machining and sanding on the processed specimens. It was done on both top and bottom. Later the roughness testing was also done in that marked region to have a very fair comparison of values. The settings used for testing can be seen in the table 5 below:

Table 5 Surface Roughness Testing Settings

Work Name	Sample	Oprator	Mitutoyo
Measuring Tool	SurfTest	Comment	Ver2.00
Standard	ISO 1997	N	5
Profile	R	Cut-Off	0.8mm
λs	2.5μm	Filter	GAUSS

The results of surface roughness testing for original specimens can be seen in the table 6 below:

Table 6 Surface Roughness Values for the Original Specimens

Original Values (μm)	0 degree	30 degree	45 degree	60 dgeree	90 degree
Top Ra	2,755	3,484	2,924	3,2935	3,5665
Bottom Ra	12,863	10,333	10,4595	11,702	11,4575
Average Ra	7,809	6,9085	6,69175	7,49775	7,512
Top Rq	3,4415	4,531	3,7295	4,332	4,498
Bottom Rq	15,2055	13,6185	12,8035	14,9015	13,7715
Average Rq	9,3235	9,07475	8,2665	9,61675	9,13475
Top Rz	17,9165	23,1085	18,5415	22,86	21,7635
Bottom Rz	64,296	64,0775	55,362	67,361	60,708
Average Rz	41,10625	43,593	36,95175	45,1105	41,23575

4.1.2 Surface Roughness Testing of Processed Specimens

After that surface roughness testing was done on the processed samples to investigate how the roughness profile has been altered on processed specimens after machining and sanding. For the processed specimens machined and sanded area in the middle-reduced section was the area supposed to be tested. That processed area had quite a similar roughness profile on both the top and bottom. That is why only one sample was enough to be tested so one sample for each angle variation was tested from the processed area on the top and bottom. Then their average value was considered to be the surface roughness of that specimen. The surface roughness values for the processed specimens can be seen in the table 7 below:

Table 7 Surface Roughness Values for the Processed Specimens

Processed Values (µm)	0 degree	30 degree	45 degree	60 dgeree	90 degree
Top Ra	2,479	4,138	4,857	3,986	5,674
Bottom Ra	4,647	4,135	3,686	4,786	5,516
Average Ra	3,563	4,1365	4,2715	4,386	5,595
Top Rq	3,577	5,455	6,075	4,994	7,049
Bottom Rq	5,772	5,436	4,743	6,152	6,983
Average Rq	4,6745	5,4455	5,409	5,573	7,016
Top Rz	24,446	30,149	29,228	25,531	32,408
Bottom Rz	27,421	28,987	25,328	31,903	34,993
Average Rz	25,9335	29,568	27,278	28,717	33,7005

4.2 Tensile Cycling (load) Testing of Original Specimens

After the surface roughness testing, the fatigue life of the samples was studied and stress-strain behaviour was observed. The results obtained from this testing will be shown in this section. Two specimens of each orientation were tested and the average of the fatigue life values of the samples was considered as the fatigue life of the specimen of that orientation. Testing Parameters were set at the beginning of testing and kept constant throughout the fatigue life testing process. Predefined testing parameters for testing can be seen in the table 8 below:

Table 8 Parameters for Fatigue Testing

Properties	**Values**
Machine no.	X350-3051
Test type	Tens. Cycling (Load)
Width of the specimen	10 mm
Length of the specimen	105.6 mm
Breadth/Thickness of the specimen	4 mm
Area	40 mm^2
Target stress	8 MPa
Target force	320 N
Number of cycles	100000
Testing speed	100 mm/min
Crosshead upper limit	700 mm
Crosshead lower limit	400 mm
Start position	435.080 mm (approx.)

Some of the broken original samples can be seen in the figure 26 below:

Figure 26 Broken original specimens after fatigue life testing

4.2.1 Original Specimen 0^0

Fatigue Life:

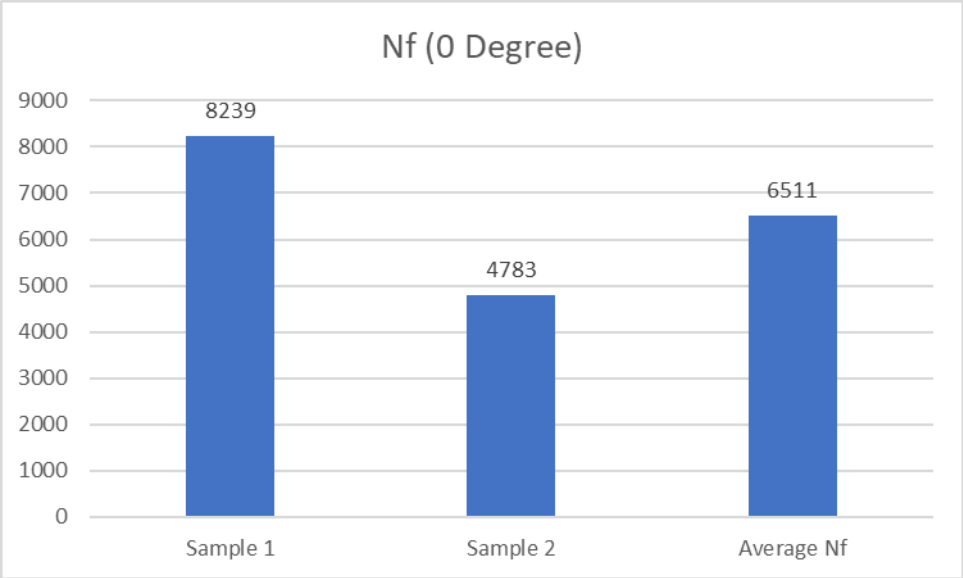

Figure 27 Fatigue Life for 0-degrees original specimen

Stress-strain Curve:

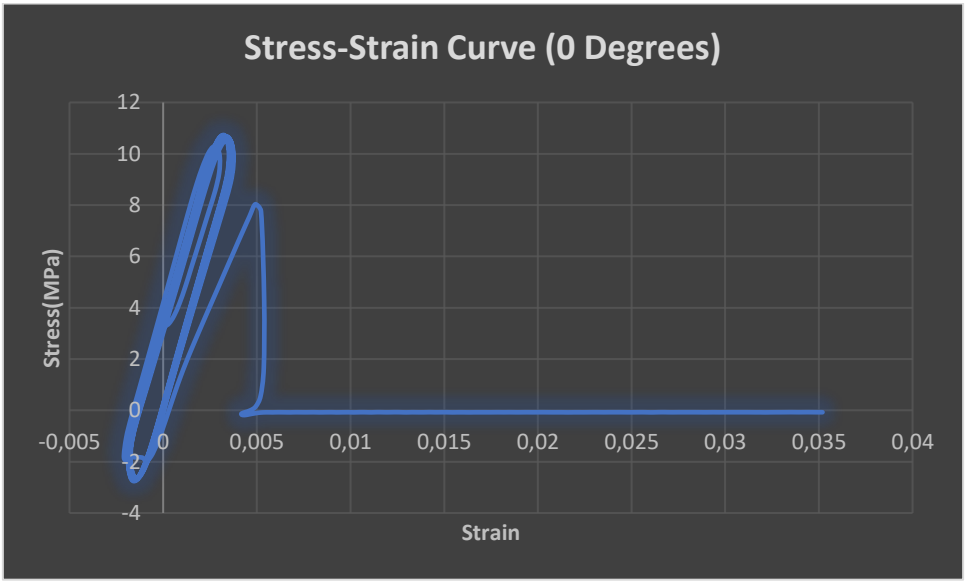

Figure 28 Stress-strain curve for 0-degrees original specimen

4.2.2 Original Specimen 30^0

Fatigue Life:

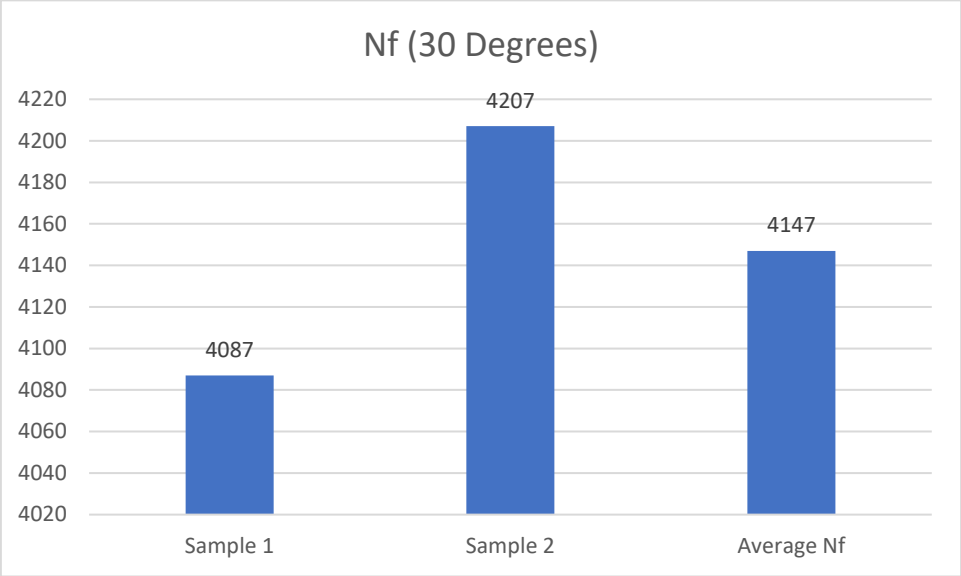

Figure 29 Fatigue Life for 30-degrees original specimen

Stress-strain Curve:

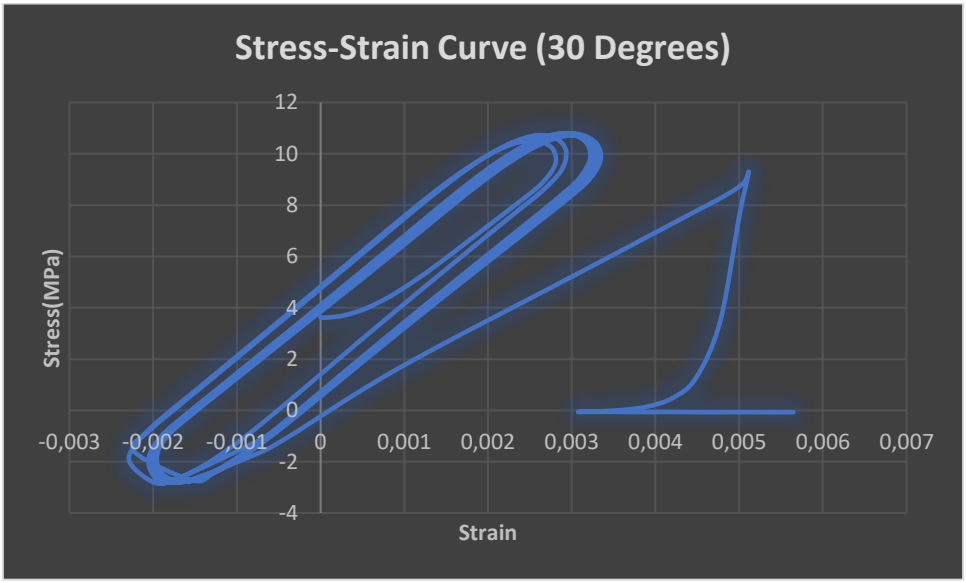

Figure 30 Stress-Strain Curve for 30-degrees original specimen

4.2.3 Original Specimen 45^0

Fatigue Life:

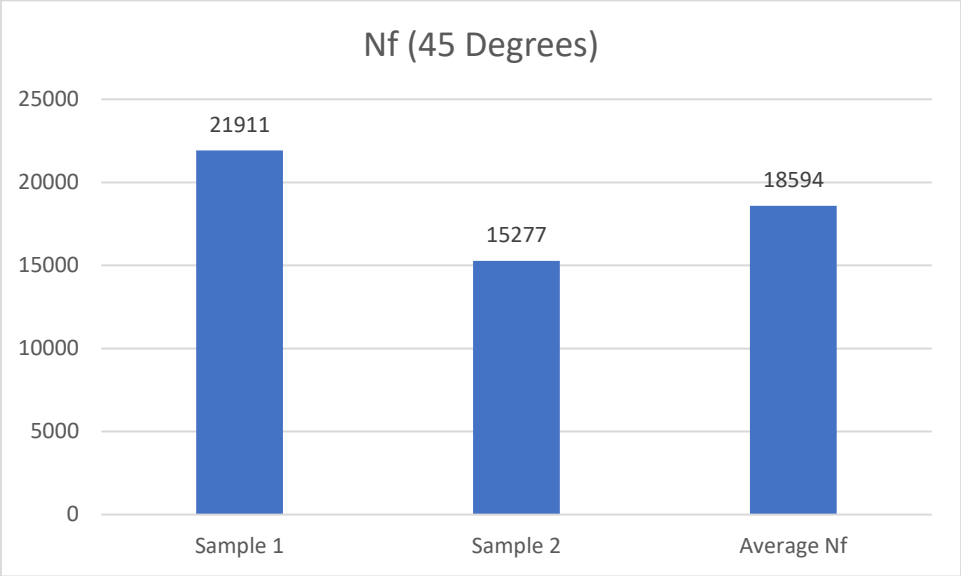

Figure 31 Fatigue Life for 45-degrees original specimen

Stress-strain Curve:

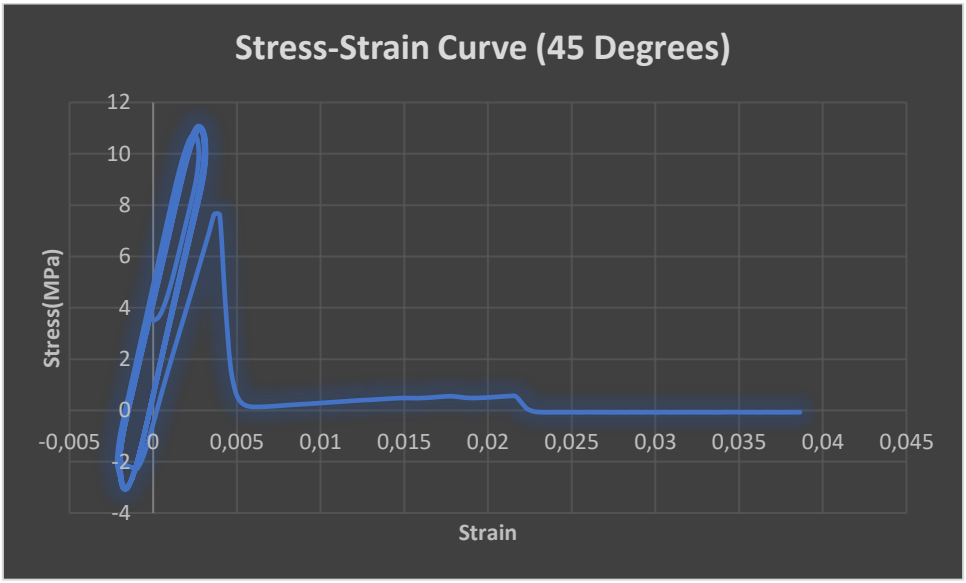

Figure 32 Stress-Strain Curve for 45-degrees original specimen

4.2.4 Original Specimen 60^0

Fatigue Life:

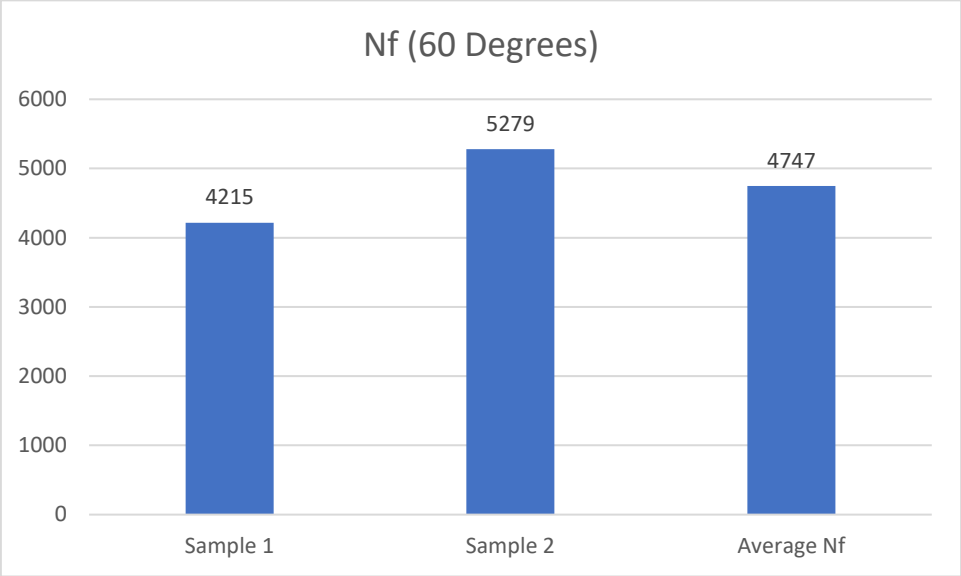

Figure 33 Fatigue Life for 60-degrees original specimen

Stress-strain Curve:

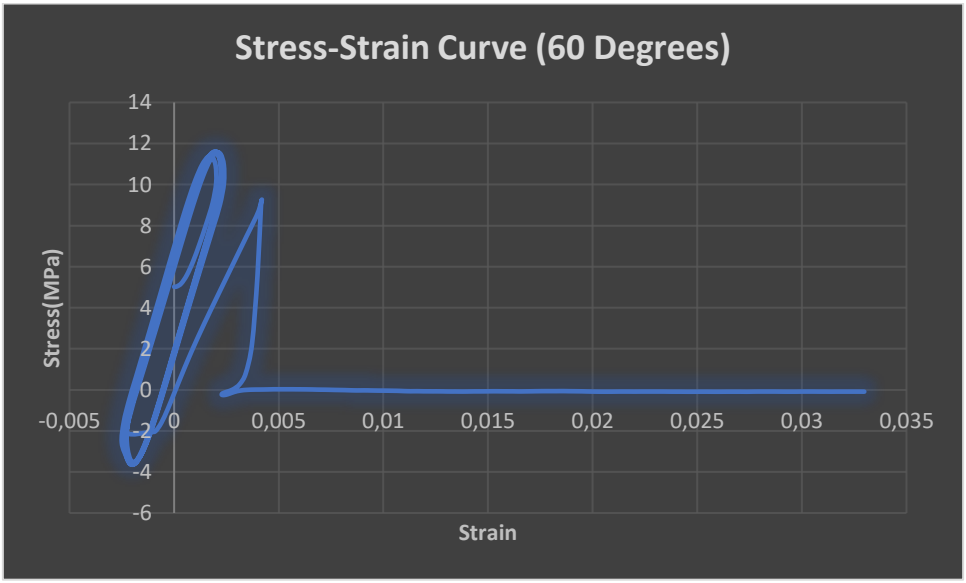

Figure 34 Stress-Strain Curve for 60-degrees original specimen

4.2.5 Original Specimen 90^0

Fatigue Life:

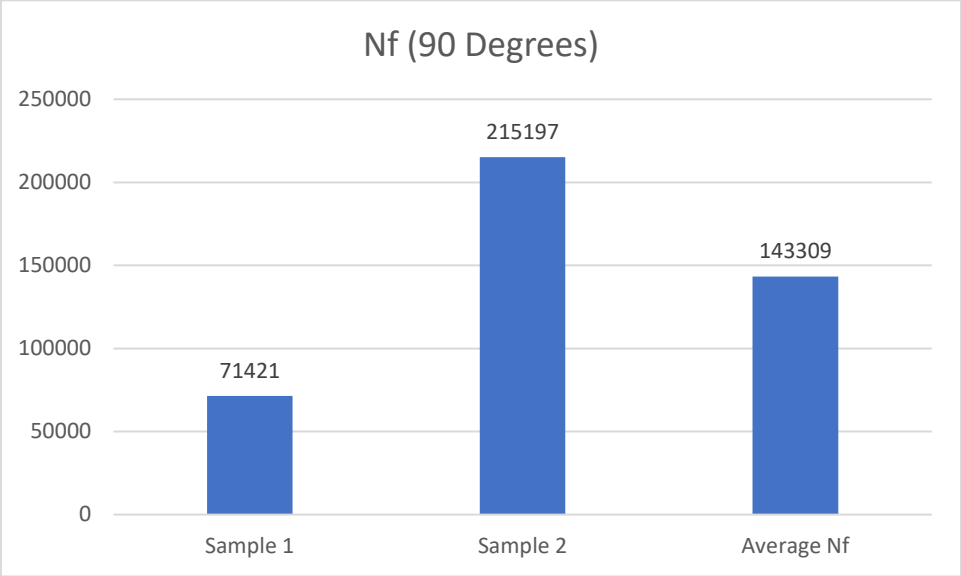

Figure 35 Fatigue life for 90-degrees original specimen

Stress-strain Curve:

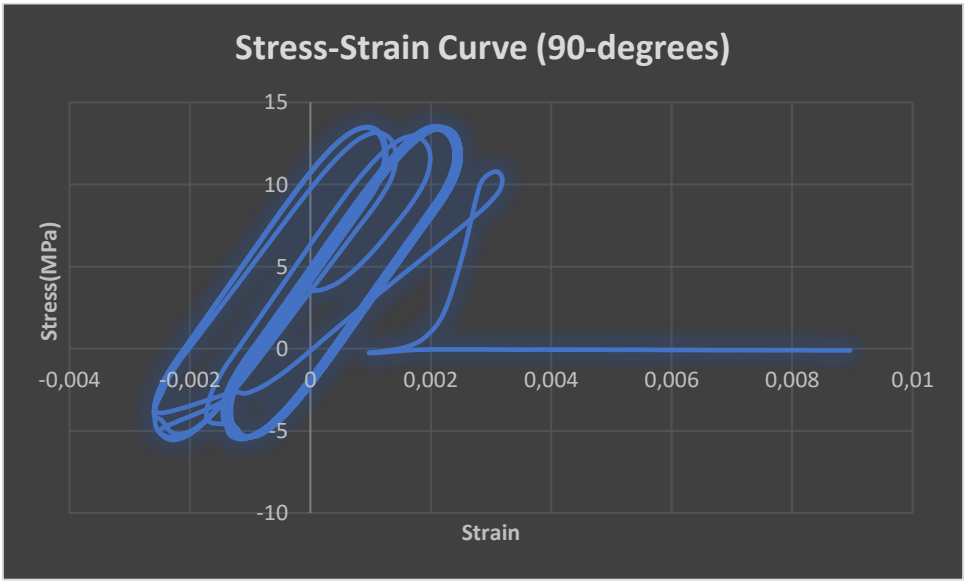

Figure 36 Stress-Strain Curve for 90-degrees original specimen

4.3 Tensile Cycling (load) Testing of Processed Specimens

After the testing of the original specimens, testing of processed specimens was done using the same testing parameters to investigate the fatigue lives of the processed specimens. Their stress-strain behaviour was also studied. The picture of broken processed specimens is shown in figure 37 below:

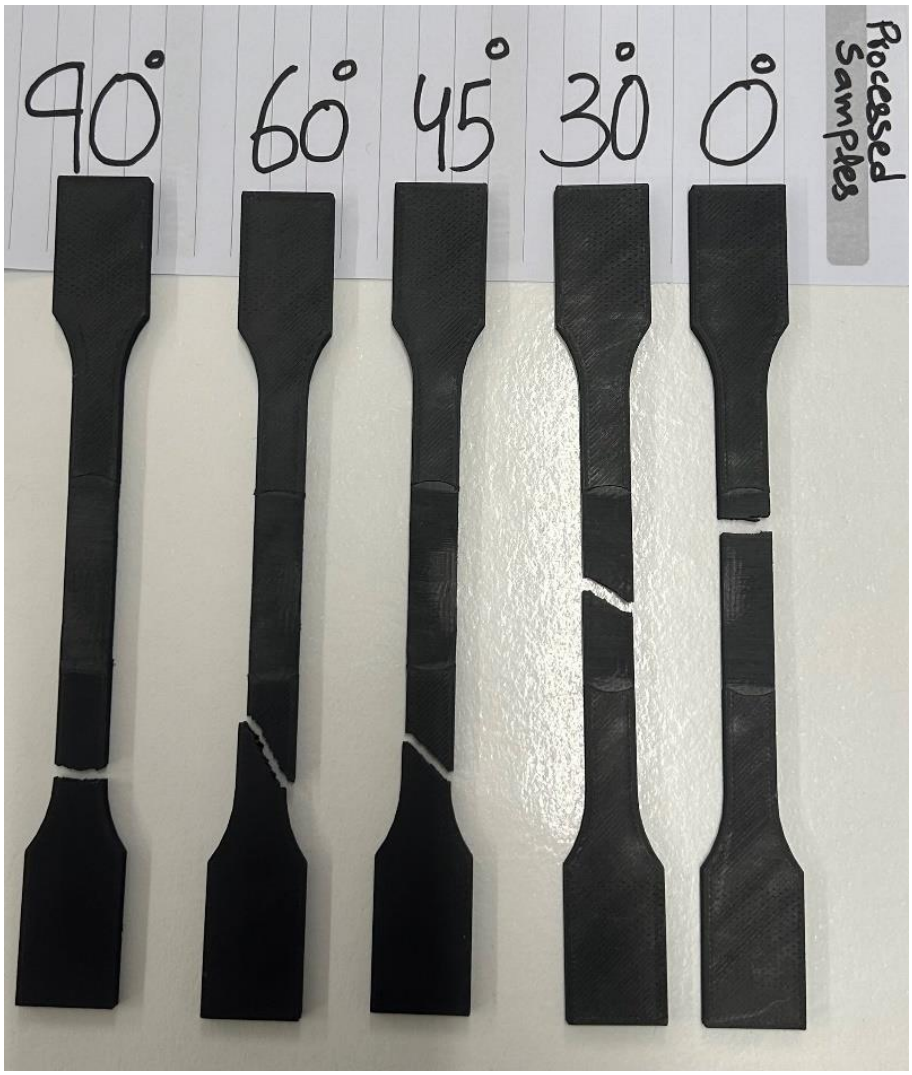

Figure 37 Broken processed specimens after fatigue testing

4.3.1 Processed Specimen 0^0

Fatigue Life:

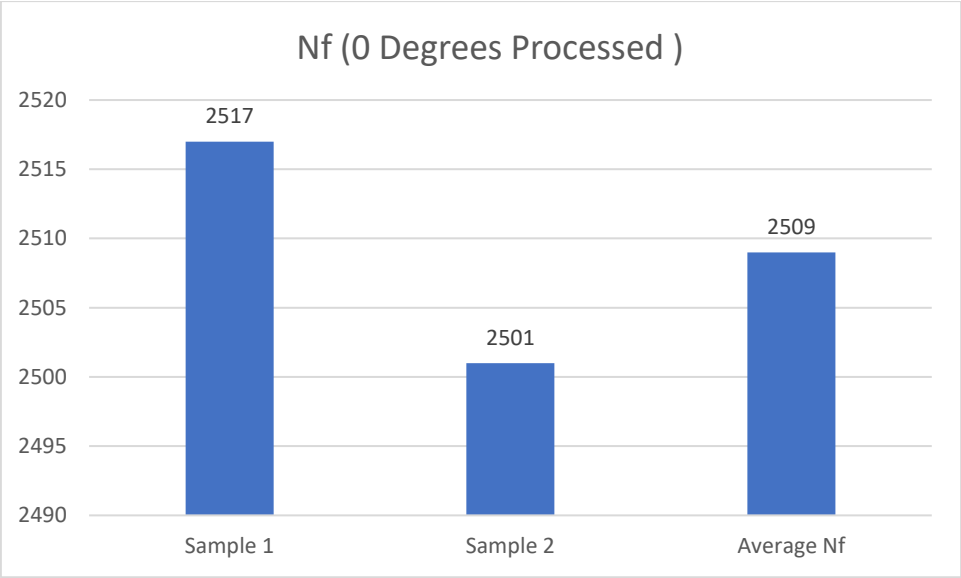

Figure 38 Fatigue life for 0-degrees processed specimen

Stress-strain Curve:

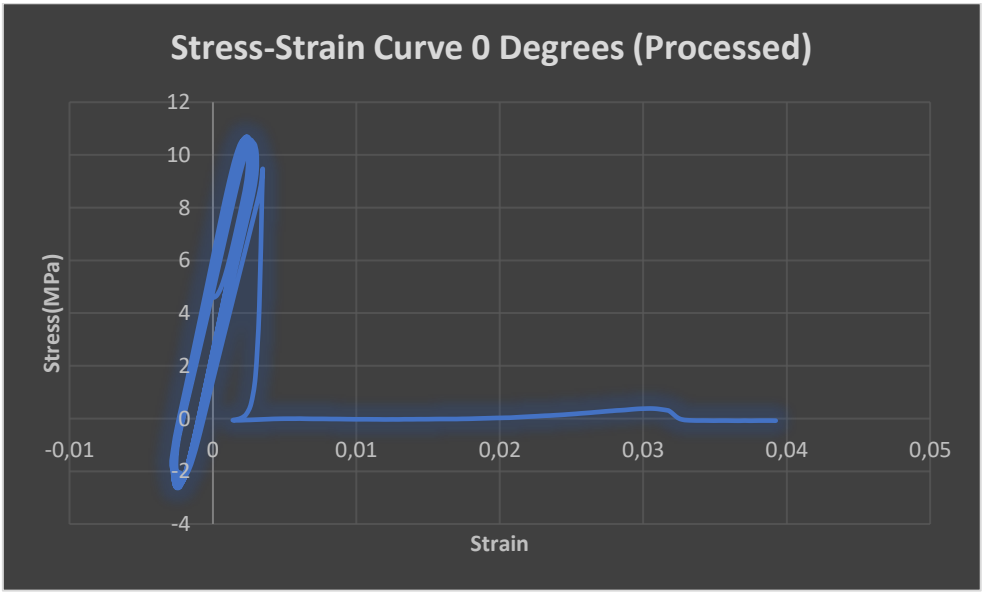

Figure 39 Stress-Strain Curve for 0-degrees processed specimen

4.3.2 Processed Specimen 30^0

Fatigue Life:

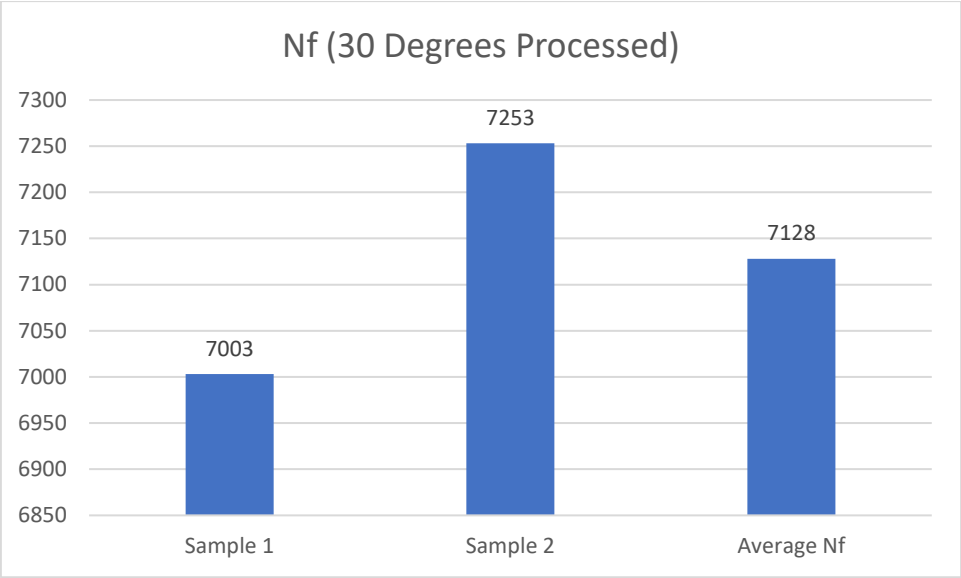

Figure 40 Fatigue life for 30-degrees processed specimen

Stress-strain Curve:

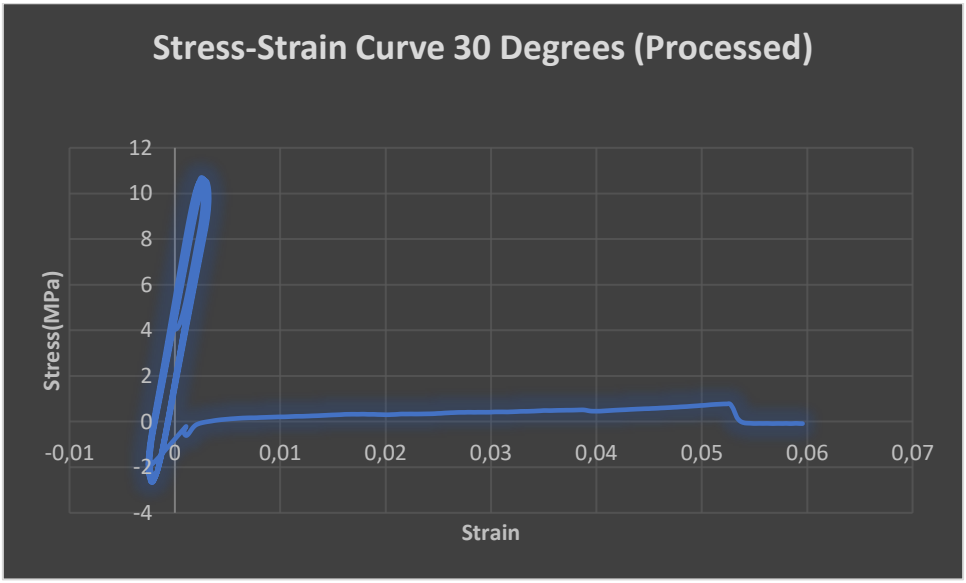

Figure 41 Stress-Strain Curve for 30-degrees processed specimen

4.3.3 Processed Specimen 45^0

Fatigue life:

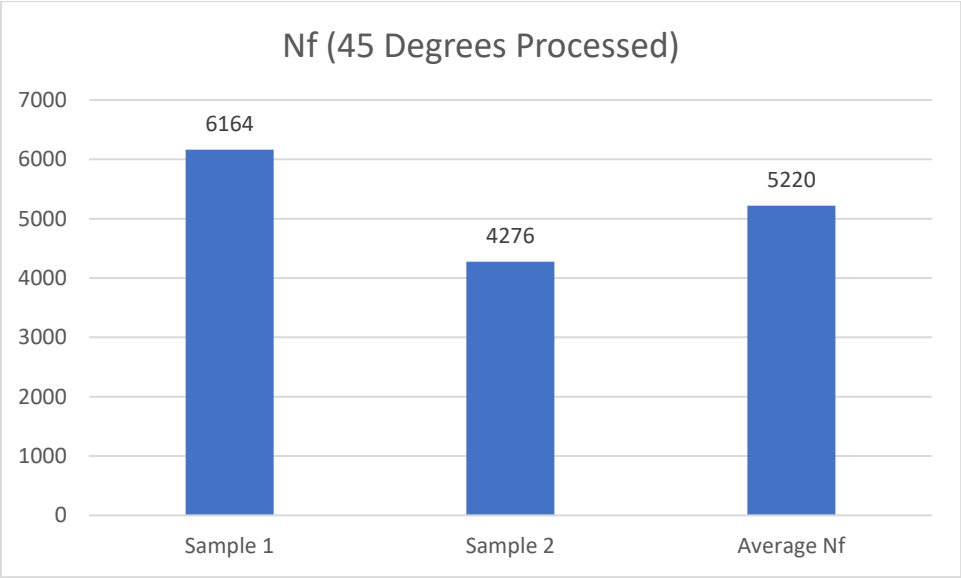

Figure 42 Fatigue life for 45-degrees processed specimen

Stress-strain Curve:

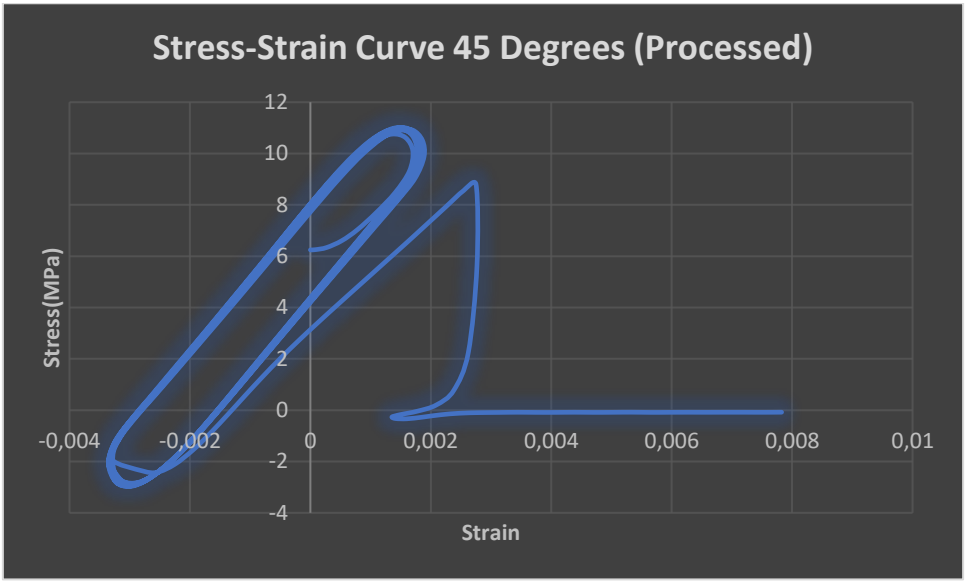

Figure 43 Stress-Strain Curve for 45-degrees processed specimen

4.3.4 Processed Specimen 60^0

Fatigue life:

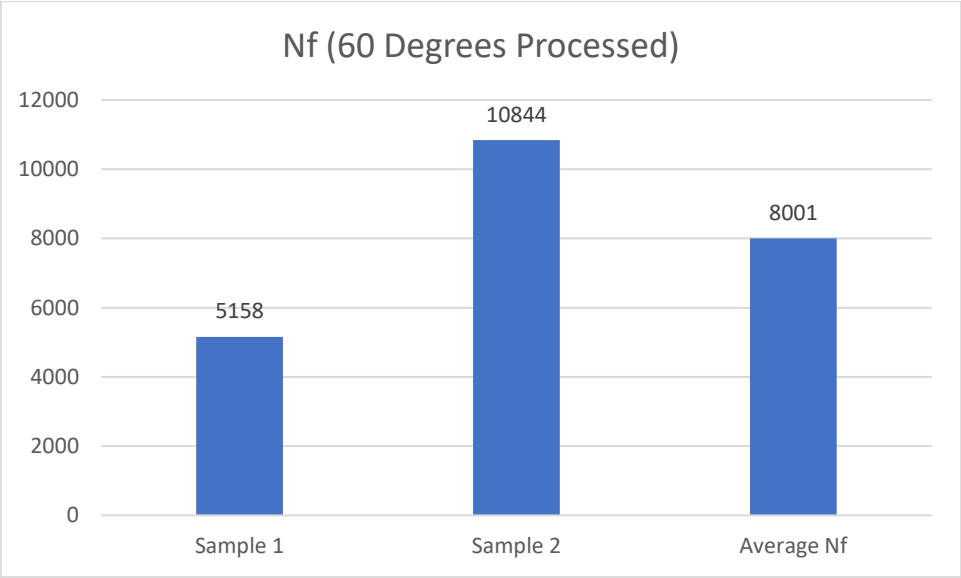

Figure 44 Fatigue life for 60-degrees processed specimen

Stress-strain Curve:

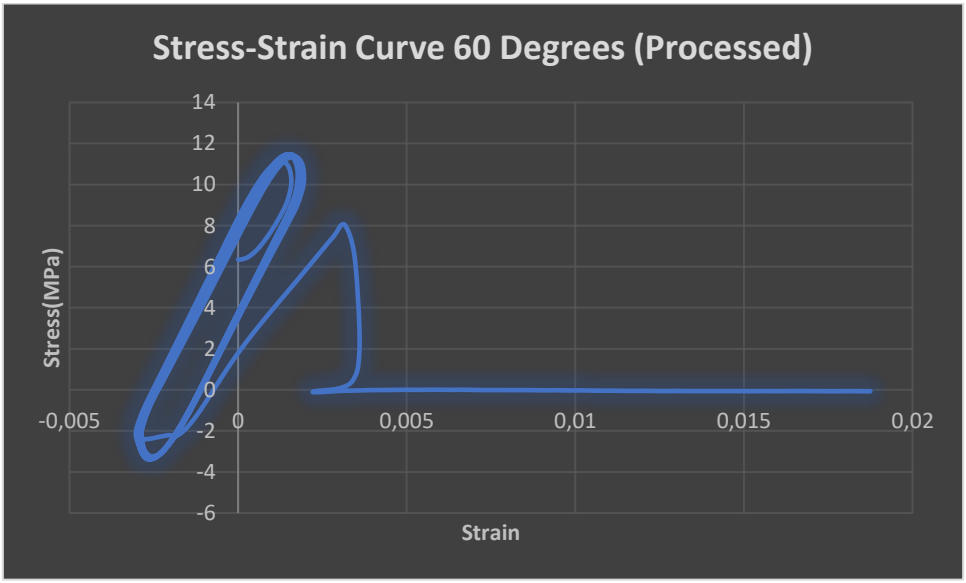

Figure 45 Stress-Strain Curve for 60-degrees processed specimen

4.3.5 Processed Specimen 90^0

Fatigue life:

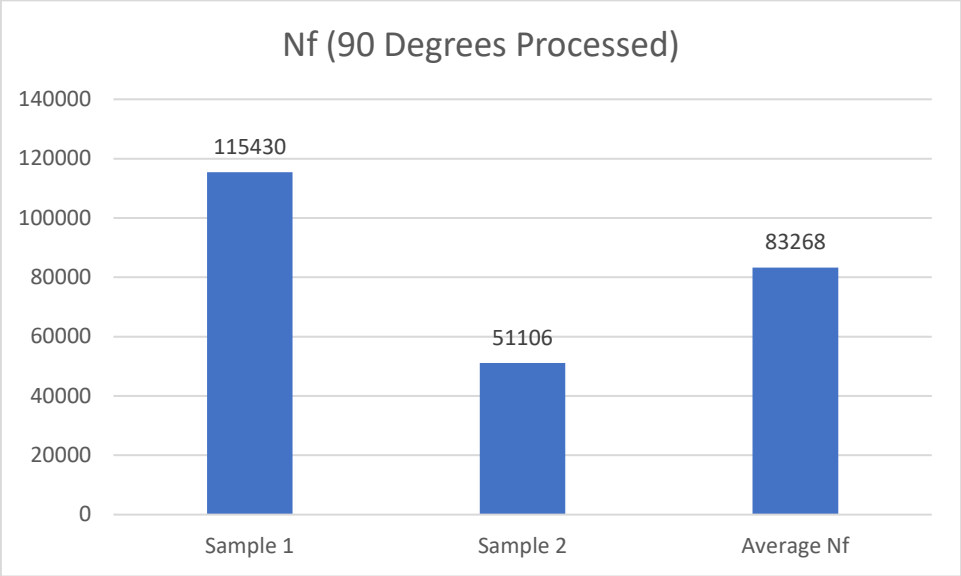

Figure 46 Fatigue life for 90-degrees processed specimen

Stress-strain Curve:

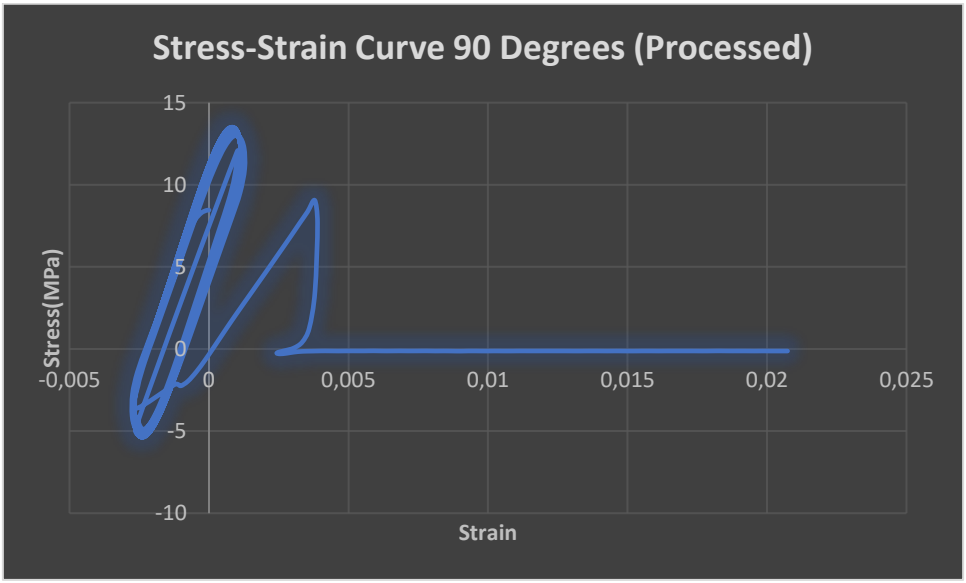

Figure 47 Stress-Strain Curve 90-degrees processed specimen

5. DISCUSSION

5.1 Influence of Infill Orientation on the Fatigue Life of Original Specimens

In figure 48 below, it can be seen how the fatigue life of the original specimens varies for the specimens having various infill orientations:

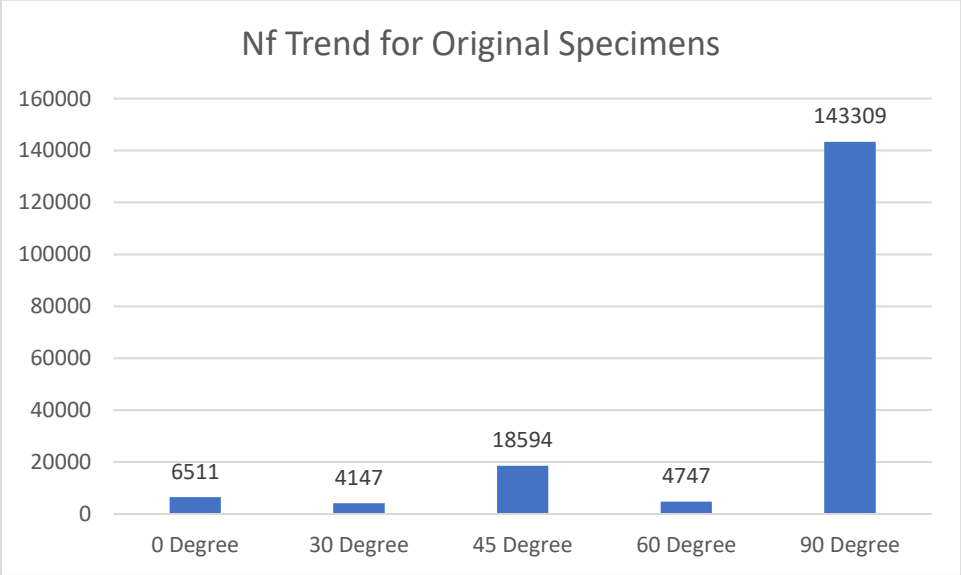

Figure 48 Fatigue life trend for original specimens

It can be seen from the figure 48 above that for original specimens 30-degrees specimen survived least for about 4147 cycles, then 60 degrees was quite close it survived for 4747 cycles. 0 degrees managed to survive 6511 cycles. 45 degrees was the second highest which survived for about 18594 cycles and 90-degrees orientation was proven to be the strongest during testing as it survived 143309 fatigue cycles. Trend is quite non-linear as fatigue life is decreasing from 0 to 30 degrees, then increasing till 45 degrees. For 60 degrees it again decreased and finally increased for 90 degrees. In fatigue life testing, the specimen is getting stretched generally in vertical direction. Which makes it harder to resist the force impact due to stretching, when the specimen is printed in a perpendicular direction such as 0^0. That is why minimum number of cycles were expected from 0 degrees or 30 degrees. The possible explanation for 90 degrees specimen having maximum number of cycles survived is that it was getting stretched vertically in the same direction of infill orientation which makes it easier for it to resist breakage for a longer time. Figure 26 shows that all of the original specimens broke from almost same point,

the potential reason for it could be the starting position for printing was same for all specimens which made that specific area more prone to breakage than others.

5.2 Variation of Surface Roughness between the Original and Processed Specimens

In the figure 49 below the difference between the surface roughness values of the original and processed specimens is shown:

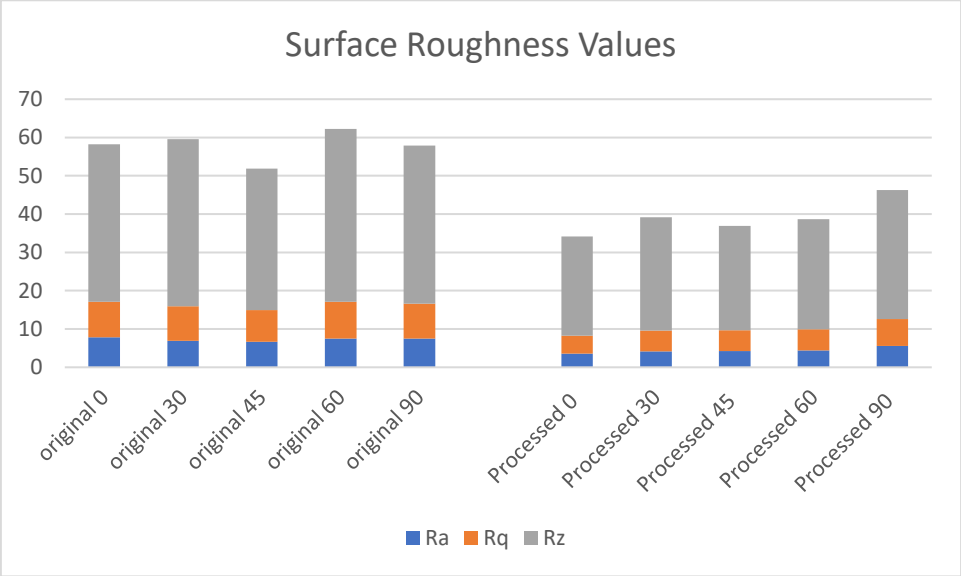

Figure 49 Surface Roughness comparison between the original and processed specimens

It can be seen from the figure 49 above that for all specimens irrespective of infill orientation surface roughness values are generally decreasing. Figure 49 also shows that Rz value for 45 degrees original specimen was deviating a bit from the average values of other orientations but for processed 45 degrees specimen, deviation was comparatively less. Processed samples have lower surface roughness values than the original samples. So, after getting machined and sanded the surface roughness values of all the samples have significantly decreased. The surfaces of 3D printed objects are quite rough or uneven as they are made of several printing layers sandwiched upon each other. After getting machined and sanded some of the upper layers were faded away which made surface even, resulting in a significant decrease in surface roughness.

5.3 Influence of Infill Orientation on the Fatigue Life of Processed Specimens

In the figure 50 below it can be seen how the fatigue life of processed specimens varies for the specimens of various infill orientations:

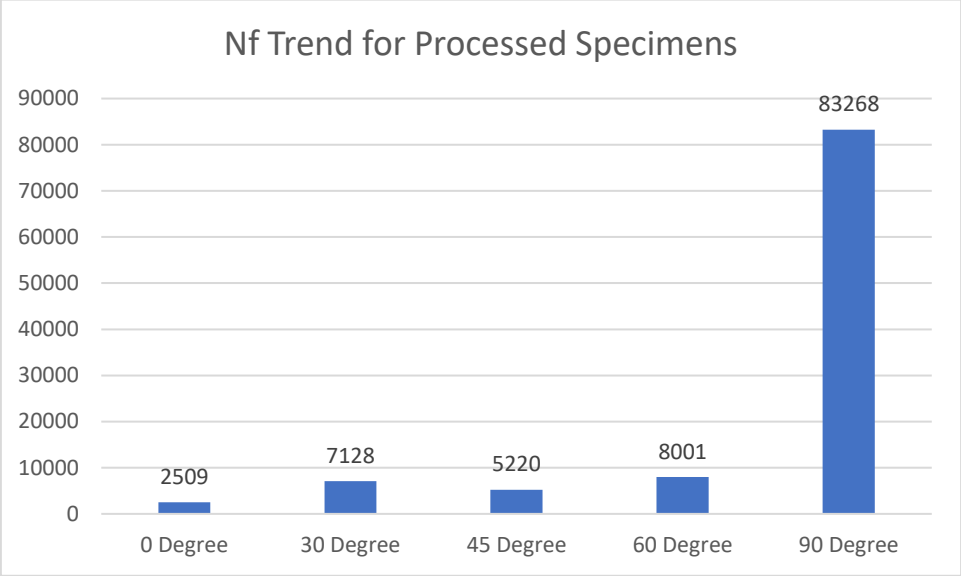

Figure 50 Fatigue life trend for the processed specimens

For processed specimens, the 0-degrees specimen appears to be the weakest as it survived only 2509 cycles. 30-degrees specimen survived 7128 cycles and 45 degrees survived 5220 cycles. 60 degrees showed to have the second highest number of cycles surviving 8001 cycles and again also for processed specimens, 90 degreess has proven to be the strongest which survived 83268 cycles. 0 degrees survived least number of cycles because it is easier to break as those samples were facing stress from perpendicular direction which makes it easier to reduce the bonding between the layers. It can be noticed from figure 37 that the 0 degrees specimen broke horizontally which means that different layers have been separated from each other. Whereas for 90 degreess, they were getting stretched vertically in the same direction as infill orientation which makes it easier for the sample to bear more cycles.

5.4 Influence of Surface Processing on the Fatigue Life of the Specimens

In the figure 51 below the fatigue lives of both original and processed specimens are compared to study how a decrease in surface roughness due to processing has influenced the fatigue life of the processed specimens:

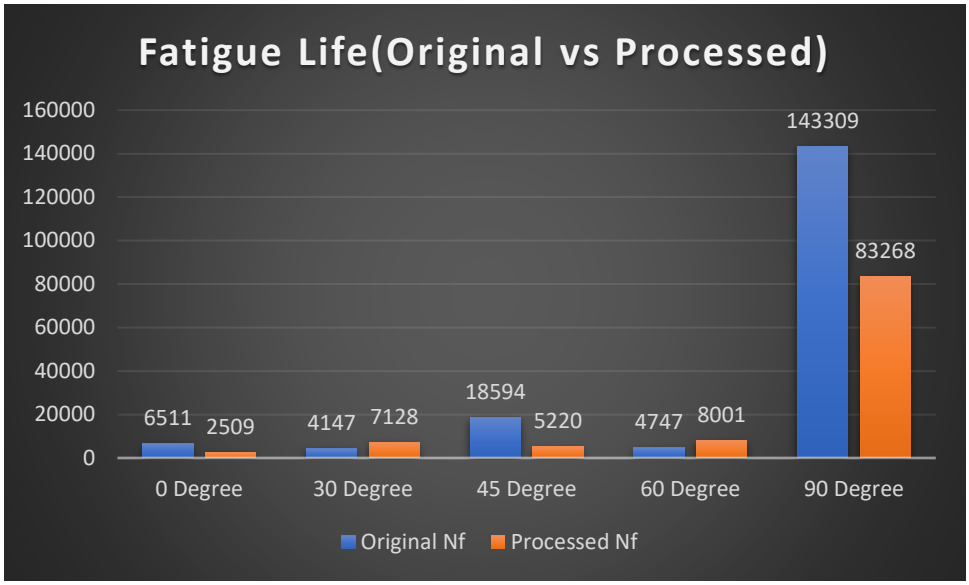

Figure 51 Fatigue Life comparison between the original and processed specimens

It can be clearly seen from the figures above that the surface roughness of the specimens has generally decreased after processing but when compared, their fatigue lives do not show any linear trend as the values are decreasing and then increasing. For the 0 degrees specimen, the fatigue life has decreased after processing from 6511 to 2509. For 30 degrees, it has increased from 4147 to 7128. In the case of 45 degrees, it has significantly decreased from 18594 to 5220. For 60 degrees, it has increased from 4747 to 8001. 90-degrees specimens had proven to be the strongest in both cases but after processing, fatigue life for 90 degrees has decreased from 143309 to 83268. This trend is quite non-linear because fatigue life depends on the variety of factors such as bonding between the material, material properties, grain size, stresses, design geometry and surface quality (Xin, 2013). There can be various reasons for variation in these values of fatigue lives such as defects inside the material, porosities, different fibre orientations or weak bonding. Although the processing and testing parameters were kept constant, yet any linear trend can not be observed.

5.5 Variation of Percentage Strain at Break for all Specimens

In the figure 52 below it can be seen how the percentage strain at the point of breaking varies for all original and processed specimens:

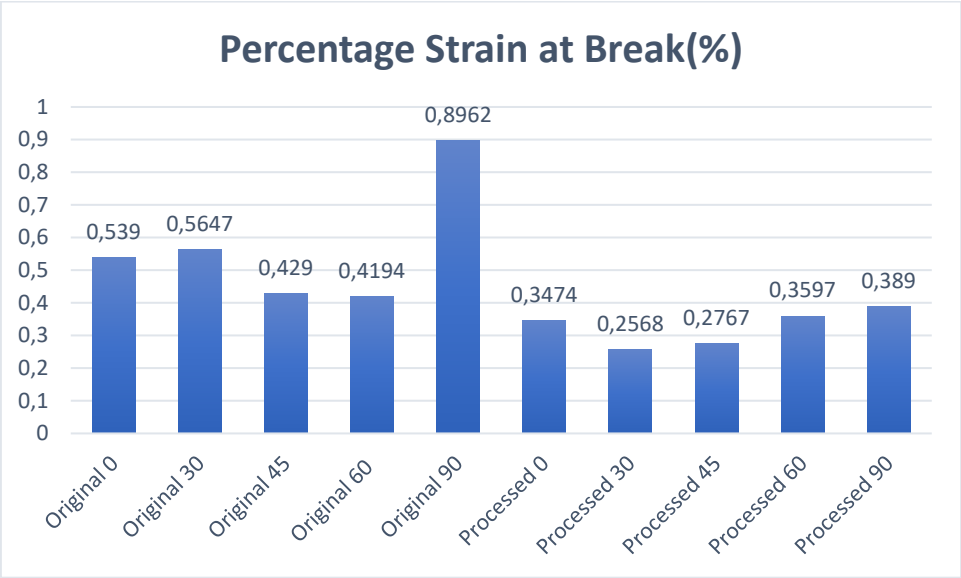

Figure 52 Strain at break comparison between the original and processed specimens

The figure 52 above shows the percentage strain at the point of breaking. It can be noticed that the strain at break for processed specimens is significantly lower than the original specimens for all orientations, this shows that strain at break generally decreased after processing for all infill orientations. The possible reason for it could be that while processing, samples were machined and sanded which means some of the layers from the surface had been faded away leaving the sample bit weaker. The thickness of the middle-reduced section of the specimen reduced further which made it feasible to break the sample at a lower strain.

5.6 Relevance to the Similar Studies

This study is quite detailed and comprehensive when compared to similar studies in this area of research. There was similar research done, (Rana, 2022) focusing on the influence of infill direction on the low cycle fatigue testing of 3D printed PLA polymer also concluded that the 90-degrees samples are showing to have the highest fatigue life. This shows that not only for this material but for even similar materials, additively manufactured samples are proven to be strongest when printed with 90 degrees infill orientation. Another article (The fatigue of Carbon Fibre Reinforced Plastics - A Review 2019) mentions that fatigue damage mechanisms for composites are highly complex

because the composite materials are intrinsically inhomogeneous. Fatigue is usually characterized by the initiation of crack and the growth of damage. This can be the potential reason behind some of the abnormal trends while testing the fatigue life of carbon fibre-reinforced material. The direction of the fibres inside the material and the presence of minor microscopic porosities affects the fatigue life of the specimen as well. Thesis done at Arcada (Tran, 2019) also studied the effects of printing parameters on tensile properties, but it used simple PLA rather than any composite polymer material.

6. CONCLUSION

In this thesis Carbon Fibre Reinforced Polyester was used as a material and using it, tensile test specimens were 3D printed using FDM technology. Specimens were designed according to the dimensions of ISO 527-2/1A. Specimens were printed in various infill orientations (0^0,30^0,45^0,60^0,90^0) and their fatigue testing was done to study how infill orientation influences the fatigue life of this material. Another set of similar samples was processed using machining and sanding to alter its surface roughness, then it was also fatigue tested. Finally, the fatigue testing data of both processed and original specimens was compared to investigate how the processing has influenced the fatigue lives of the specimens with various infill orientations.

After analyzing the series of figures in the results section various conclusions can be derived from the experimental work of this thesis. From figure 48, it can be observed that the 90-degrees specimen has proven to be the strongest among the original specimens. Figure 49 shows the clear trend that the surface roughness for all the samples with all infill orientations has generally decreased as a result of machining and sanding. Figure 50 shows that even for the processed specimens, 90 degrees has proven to be the strongest. So, it can be concluded that specimens are strongest when additively manufactured using a 90-degrees infill orientation. It can be observed from figure 51 that when fatigue lives of original and processed specimens were compared, they do not show any linear trend. For 0, 45 and 90 degrees, fatigue life is decreased. Whereas for 30 and 60 degrees, it has increased. In figure 52, percentage strain at break is compared for all original and processed specimens. It can be clearly noticed that the percentage strain at

break has decreased after processing for every angle orientation. So, it can be deduced that strain at break decreases with a decrease in surface roughness.

In a nutshell, this thesis managed to fulfil its research objectives. It has been analyzed through testing and data analysis of obtained data that how various infill orientations affect the fatigue life of this material. It is also shown through various fatigue performance comparisons that how surface machining and sanding influences the fatigue life of this material. Fatigue life is a very important property as it defines the durability of the product. It is also crucial to know which angle orientation can offer the strongest possible specimen to be used in various applications. Conclusively, after a series of testing, it has been found that a specimen of this material is proven to be strongest when additively manufactured with a 90-degrees infill orientation. Moreover, through a series of figures, the influence of surface machining and sanding on the fatigue performance of this material has also been explained.

REFERENCES

A complete guide to understand surface roughness in manufacturing - LEADRP - rapid prototyping and manufacturing service (2022) *LEADRP*. Available at: https://leadrp.net/blog/a-complete-guide-to-understand-surface-roughness-in-manufacturing/ (Accessed: April 12, 2023).

Additive manufacturing history: From the 1980's to now (no date) Markforged. Available at: https://markforged.com/resources/blog/additive-manufacturing-history (Accessed: March 4, 2023).

Alam, P. et al. (2019) 'The fatigue of Carbon Fibre Reinforced Plastics - A Review', Composites Part B: Engineering, 166, pp. 555–579. doi:10.1016/j.compositesb.2019.02.016.

Am basics (2022) Additive Manufacturing (AM). Available at: https://additivemanufacturing.com/basics/ (Accessed: March 4, 2023).

Du, Y. et al. (2022) "High-throughput screening of surface roughness during additive manufacturing," Journal of Manufacturing Processes, 81, pp. 65–77. Available at: https://doi.org/10.1016/j.jmapro.2022.06.049.

Ender-3 S1 Pro 3D Printer (no date) creality. Available at: https://www.creality.com/products/creality-ender-3-s1-pro-fdm-3d-printer (Accessed: April 30, 2023).

Jung, C.-ho et al. (2022) "Ultrasonic fatigue analysis of 3D-printed carbon fibre reinforced plastic," Heliyon, 8(11). Available at: https://doi.org/10.1016/j.heliyon.2022.e11671.

(No date a) X350 - inquality. Available at: https://inquality.gr/wp-content/uploads/2020/10/X350-Range.pdf (Accessed: 04 June 2023).

Parandoush, P. and Lin, D. (2017) 'A review on additive manufacturing of polymer-fibre composites', Composite Structures, 182, pp. 36–53. doi:10.1016/j.compstruct.2017.08.088.

Rahman, R. (2019) Tensile property, Tensile Property - an overview | ScienceDirect Topics. Rozyanty Rahman, Syed Zhafer Firdaus Syed Putra. Available at:

https://www.sciencedirect.com/topics/materials-science/tensile-property (Accessed: April 2, 2023).

Rana, M. (2022) The influence of infill direction on the low cycle fatigue performance of 3D printed PLA polymer., Theseus. Available at: https://www.theseus.fi/handle/10024/788533 (Accessed: January 30, 2023).

Ralls, A.M. et al. (2022) "Development of surface roughness from additive manufacturing processing parameters and postprocessing surface modification techniques," Tribology of Additively Manufactured Materials, pp. 193–222. Available at: https://doi.org/10.1016/b978-0-12-821328-5.00007-x.

Rouf, S. et al. (2022) '3D printed parts and mechanical properties: Influencing parameters, sustainability aspects, global market scenario, challenges and applications', Advanced Industrial and Engineering Polymer Research, 5(3), pp. 143–158. doi:10.1016/j.aiepr.2022.02.001.

Samples with printing orientations 0 • , 30 • , 45 • , 60 • and 90 (no date). Available at: https://www.researchgate.net/figure/Samples-with-printing-orientations-0-30-45-60-and-90-The-horizon-lines_fig2_330209714 (Accessed: April 16, 2023).

Special cases of fluctuating stresses (no date) Ques10. Available at: https://www.ques10.com/p/42980/special-cases-of-fluctuating-stresses/ (Accessed: April 13, 2023).

Stress and strain (no date) Nondestructive Evaluation Physics : Materials. Available at: https://www.nde-ed.org/Physics/Materials/Mechanical/StressStrain.xhtml (Accessed: April 2, 2023).

SURFTEST SJ-410 series (2022) Mitutoyo. Available at: https://www.mitutoyo.com/literature/surftest-sj-410-series/ (Accessed: May 7, 2023).

The best 3D printer settings for perfect prints (2022) All3DP. Available at: https://all3dp.com/2/3d-slicer-settings-3d-printer/ (Accessed: April 30, 2023).

Tran, N. (2019) The impact of printing orientation on the tensile properties of parts printed by fused deposition modelling, Theseus. Tran, Nhu. Available at: https://www.theseus.fi/handle/10024/266328 (Accessed: February 16, 2023).

What is FDM (fused deposition modeling) 3D printing? (no date) Hubs. Available at: https://www.hubs.com/knowledge-base/what-is-fdm-3d-printing/ (Accessed: March 4, 2023).

What is fatigue life? (2023) Metal Fatigue Life Prediction. Available at: https://fatigue-life.com/what-is-fatigue-life/ (Accessed: April 12, 2023).

XT-CF20 (no date) High-Quality 3D Printing Filaments for Professionals and Hobbyists. Available at: https://colorfabb.com/xt-cf20 (Accessed: April 25, 2023).

Xin, Q. (2013) ‘Durability and reliability in diesel engine system design’, Diesel Engine System Design, pp. 113–202. doi:10.1533/9780857090836.1.113.

Young's Modulus (2023) Encyclopædia Britannica. Encyclopædia Britannica, inc. Available at: https://www.britannica.com/science/Youngs-modulus (Accessed: April 12, 2023).